University of Alberta

Hyperbranched Phosphorylcholine Polymers Synthesized via RAFT Polymerization for Gene Delivery and Synthesis of an Elastomeric Conductive Polymer for Cardiovascular Applications

by

Manraj Jawanda

A thesis submitted to the Faculty of Graduate Studies and Research

in partial fulfillment of the requirements for the degree of

Master of Science

in

Process Control

Department of Chemical and Materials Engineering

Fall 2012

Edmonton, Alberta

Abstract

Gene therapy has the potential to treat a variety of hereditary diseases and relies on the design of a delivery system which can carry a gene of interest into a cell. Viruses were the standard for gene delivery and showed high cell transfection, but could induce an immunological response. As a result, there has been a growing interest towards non-viral carriers such as polymers which are less toxic. This study focused on the synthesis of a hyperbranched phosphorylcholine that incorporates a nontoxic and biocompatible poly(2-Methacryoyloxyethyl Phosphorylcholine (MPC)). The hyperbranched copolymers were synthesized via RAFT polymerization and showed broad molecular weight distributions. However the gene expression was found to be significantly lower than the current non viral standard.

In the second part of this thesis, conductive materials were embedded into elastomer films. In this study, two conductive materials: Poly(p-phenylene vinylene) (PPV) and Multi-Walled Carbon Nanotubes (MWNT) were embedded into Polydimethylsiloxane (PDMS).

Acknowledgement

I would like to thank my supervisor Dr. Ravin Narain for giving me the opportunity to work in his lab. With his advice, I have learned about the hard work required in the lab and thorough understanding of concepts which is expected from people in the scientific community.

I would like to thank Dr. Eric Flaim from the University of Alberta Nano Fabrication Lab for helping me with my PPV synthesis.

I would like to thank all of my colleagues in the lab for their patience and guidance during my research in the lab.

I would also like to thank my family for their support throughout this entire endeavor.

Table of Contents

List of Tables

List of Figures

Abbreviations

RAFT: Reversible Addition-Fragmentation chain Transfer polymerization

PEI: Polyethyleneimine

MPC: 2-Methacryoyloxyethyl phosphorylcholine

AEMA: 2-Aminoethyl methacrylamide hydrochloride

poly(MPC): Poly(2-Methacryoyloxyethyl phosphorylcholine)

DNA: Deoxyribonucleic acid

MBAm: *N*,*N*'-Methylene-bis-acrylamide

BCA: Bicinchoninic acid

HEP G2: Liver Hepatocellular Carcinoma

IV: Intrinsic viscosity

GPC: Gel Permeation Chromatography

SEC: Size Exclusion Chromatography

M_n: Number average molecular weight

M_w: Weight average molecular weight

M_w/M_n: Molecular weight distribution

R_h: Hydrodynamic radius

V_h: Hydrodynamic volume

V_i: Interstitial volume

V_p: Pores volume

V_e: Elution volume

RI: Refractive Index

LALLS: Low angle laser light scattering

MALLS: Multi angle laser light scattering

NMR: Nuclear Magnetic Resonance

TAE: Tris-acetate-EDTA

TBE: Tris-borate-EDTA

β-gal: Beta Galactosidase

ONPG: ortho-Nitrophenyl-β-galactosidase

ONP: ortho-Nitrophenyl

TMS: Tetramethylsilane

BME: B-mercaptoethanol

CTA: Chain Transfer Agent

CTP: Cyanopentanoic acid dithiobenzoate

ACVA: 4,4'-Azobis (4-cyanovaleric acid)

EGDMA: Ethyleneglycol Dimethacrylate

DEP: 2,2-Dimethacroyloxy-1-ethoxypropane

CHAPS: 3-[(3-Cholamidopropyl) dimethylammonio]-1-propanesulfonate

DMEM: Dulbecco's Modified Eagle Medium

DPBS: Dulbecco's modified Phosphate Buffer Saline

FBS: Fetal Bovine Serum

P/D: Polymer/DNA mass ratio

$CaCl_2$: Calcium Chlroide

PDMAPAAm: Poly(N,N-dimethylaminopropyl acrylamide)

PPV: Poly(p-phenylene vinylene)

PDMS: Polydimethylsiloxane

MWNT: Multi-walled carbon nanotubes

FTIR: Fourier Transform Infrared Spectroscopy

TGA: Thermogravimetric analysis

DMF: Dimethylformamide

THT: Tetrahydrothiophene

MS: Mass spectrometry

G': Storage modulus

E: Electric field strength

τ_{ind}: Induced time

τ_{rec}: Recovery time

TEOS: Tetraethyl orthosilicated

Part 1: Hyperbranched Phosphorylcholine Polymers Synthesized via RAFT polymerization for Gene Delivery

Introduction

This thesis is divided into three chapters:

Chapter 1 is a literature review that talks about RAFT polymerization, poly(2 Methacryloyloxyethyl Phosphorylcholine), polymer architecture, and applications of polymers in gene delivery. Reversible addition-fragmentation chain transfer polymerization (RAFT) was chosen to synthesize the copolymers. While different polymerization techniques will be discussed, particular attention will be given to the subclass of radical polymerization since it is the focus of this study. 2-Methacryloyloxyethyl phosphorylcholine (MPC) was copolymerized with a cationic monomer in this study and its general properties along with synthesis and current applications are discussed. Polymer architecture refers to how the monomers are oriented and this project was focused on hyperbranched structures. An outline of dendrimers as well as their different synthesis techniques was given before moving into hyperbranched polymers. The polymers were synthesized via RAFT polymerization and the hyperbranched structure was achieved through the incorporation of a cross linking agent. The aim of this work was to evaluate a range of tailor-made hyperbranched polymers as potential carriers for nucleic acid delivery to cells.

Chapter 2 introduces the instrumentation and experimental techniques used in this project to synthesize and characterize polymers and evaluate their performance as a gene delivery vector. Gel Permeation chromatography (GPC) was used to characterize the polymers for their molecular weights and molecular weight distribution. Nuclear Magnetic Resonance (NMR) is a characterization technique that was used to verify the

chemical structure of the polymer. Agarose Gel electrophoresis was used to determine how well the copolymer binds to DNA. Liver Hepatocellular Carcinoma (Hep G2) cells were cultured and their concentration was calculated using a hemacytometer. Transfection efficiencies were evaluated using a β-galactosidase and bicinchoninic acid (BCA) assay. 2-aminoethyl methacrylamide hydrochloride (AEMA) monomer was synthesized as previously reported and copolymerized with MPC monomer in a random configuration.

Chapter 3 focused on the results and discussion. The prepared cationic phosphorylcholine-based hyperbranched polymers had a broad molecular weight distribution. Different cross-linkers were used, however *N*,*N*'-Methylene-bis-acrylamide (MBAm) was the only cross linker that resulted in copolymers with broad molecular weight distributions. The copolymers were subsequently used in the condensation of plasmid DNA and the complexation was monitored by agarose gel electrophoresis. At a certain concentration, complete complexation of DNA was noted and the resulting polyplexes were subsequently evaluated as gene delivery vectors in Hep G2 cells.

1. Literature Review

1.1 Techniques of Polymerization

Polymers are used in a wide variety of fields and are important materials for meeting demands in specialized fields. [1] In the last decade, polymers have broadened their applications from industrial bulk materials into high technology fields such as: nanotechnology, optics and biomaterials. [2]

Polymerization can be classified into two main subcategories: Chain growth polymerization and Step-wise Polymerization and is shown in Figure 1.1. Since Reversible Addition-Fragmentation Chain Transfer (RAFT) polymerization is a type of chain growth polymerization, this review will focus on this category. [1]

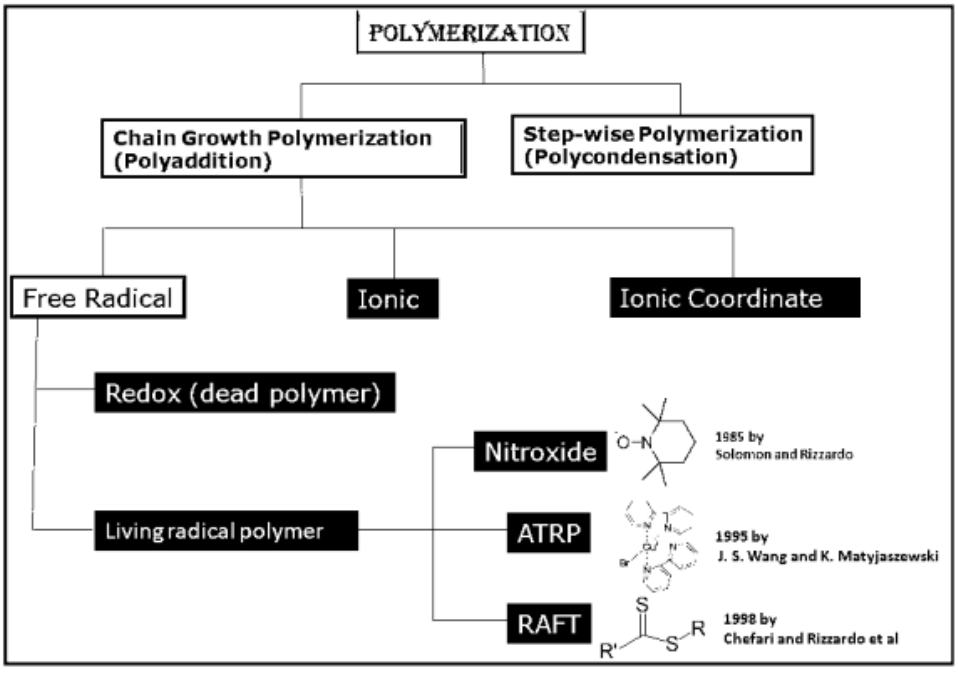

Figure 1.1: Overview of polymerization techniques [1]

Free radical polymerization is a type of chain growth polymerization. The polymer is formed from the successive addition of monomer units. The monomer is broken at the double bond which creates an active propagating radical. [3] There are three distinct steps in free radical polymerizations [1]:

1. Initiation: an active site is formed on the monomer species after the initiator species breaks the monomer at the double bond.
2. Propagation: monomer molecules are added one by one at the active site which is regenerated every time.
3. Termination: Ideally, the propagation reaction should proceed until all of the monomers are used up. However, this is very unlikely. The growth of the polymer chain is usually stopped by a termination reaction which can occur in one of two ways: combination and disproportionation. Combination occurs when two propagating species join free electrons and form a single chain. Disproportionation occurs when the active site from one chain strips a hydrogen from another chain and forms a carbon double bond in place of the missing hydrogen.

Free radical polymerization has its limitations such as: little control over molecular weight distribution due to termination reactions between radicals and the inability to synthesize block copolymers or other chain topologies. [1] Living radical polymerization also known as controlled radical polymerization gives control over polymeric structural parameters through the absence of chain transfer and termination. Unlike free radical polymerization, living radical polymerization has fast initiation and ensures that nearly all

chains grow simultaneously. [5] Additionally, the polymerization only stops when all of the monomer is used up and as a result no chain is terminated prematurely. [1]

1.2 RAFT Polymerization

Reversible Additional-Fragmentation chain Transfer (RAFT) polymerization is a living polymerization technique that was first reported in 1998 by Moad, Rizzardo and Thang. RAFT is referred to as living polymerization because it provides unprecedented control over molecular weight, molecular weight distributions, composition and architecture. [5] RAFT can be used for a wide variety of monomers and there have been many publications which have shown the versatility of RAFT in both homogenous and heterogeneous environments. [3]

RAFT uses a chain transfer agent (CTA) which allows for the controlled growth of polymer chains and can result in the synthesis of uniform chain lengths , an interesting and useful feature which was unavailable amongst other polymerization techniques.[2] Equation 1 can be used to calculate the moles of CTA required to obtain a target molecular weight:

$$M_{n\,(theory)} = \left(\frac{[Monomer]_0}{[CTA]_o}\right) \times MW_{Monomer} \quad (1)$$

Figure 1.2 shows an outline of the RAFT mechanism. *Step (i)* is initiation, where an initiator decomposes into two fragments and reacts with a single monomer to yield a propagating radical P_m. *Step (ii)* is the initial equilibrium which proceeds when P_m reacts with the RAFT agent **1** and breaks the C=S bond creating a radical intermediate **2**. There

is evidence that all of the CTA's are consumed and react with P_m before any propagation takes place because of the highly reactive C=S bond which is favored over the addition of any double bonds on the monomer. [4] Subsequently, the radical intermediate **2** fragments and releases the R group. It is vital that this R group is reactive enough that it can reinitiate the monomer species and form another propagating radical P_n (*step iii* reinitiation). In *step iv*, P_n first breaks the C=S bond and creates a growing propagation radical **4**. This radical releases the other propagating radical P_m which reinitiates another monomer and *step iv* is repeated except this time P_m attacks the C=S bond and P_n is released. This process is repeated until all the monomer is used up and termination occurs.

The length of each chain is controlled by the intermediate **4.** When P_m is released, it attaches to another monomer and then attacks the C=S bond on the intermediate release the other propagating radical P_n. The propagation step ensures that each chain P_m and P_n both grow at the same rate. [4]

i Initiation

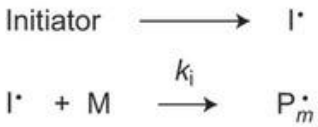

ii Initial equilibrium

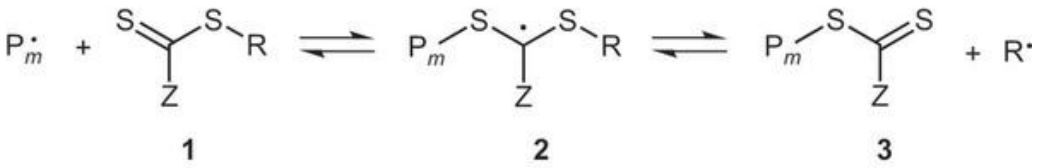

1 **2** **3**

iii Reinitiation

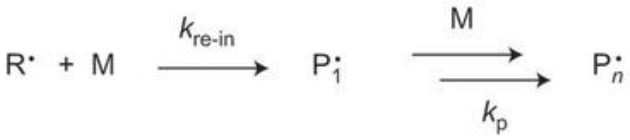

iv Main equilibrium

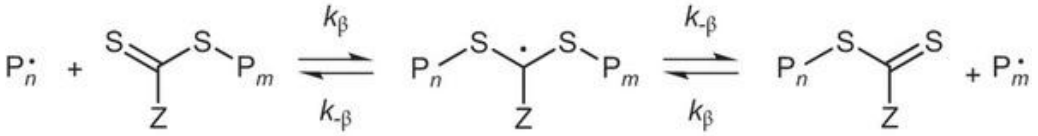

4

v Termination

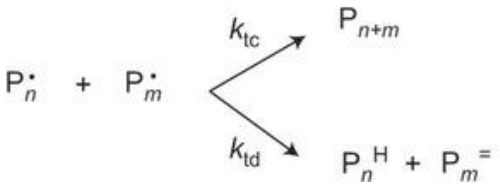

Figure 1.2: RAFT Mechanism [4]

The chain transfer agent is shown in Figure 1.3. CTA's are classified based on the nature of the Z group: dithiobenzoates, xanthates, dithiocarbamates and trithiocarbonates.

The Z group determines the rate of radical addition and also the lifetime of the intermediate CTA. The R group should be a good leaving group and also be able to reinitiate free monomers.

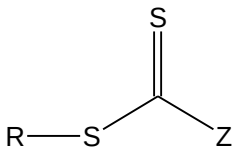

Figure 1.3: Structure of the chain transfer agent

1.3 2- Methacryloyloxyethyl Phosphorylcholine

Phosphorous containing monomers have been the subject of much interest because of their unique properties. The different positions and orientations of the phosphorous atoms on the given monomer dictates the final properties and hence, the applications in a wide variety of fields. The polymers have been used in applications such as fire extinguishers and in alternative energy production like proton conducting fuel cell membranes. Until very recently, phosphorous based materials have started to move their way into the biomedical field because of characteristics such as biodegradability, blood compatibility, reduced protein adsorption and strong interactions with dentin, and enamel. These characteristics are helping phosphorous based materials broaden their applications into tissue engineering, drug delivery and dentistry. [6]

A new phosphorous based polymer named poly(2- Methacryloyloxyethyl Phosphorylcholine) (poly(MPC)) has started to gain much attention in the biomedical field. The structure of the MPC monomer is shown in Figure 1.4 and shows the phospholipid group.

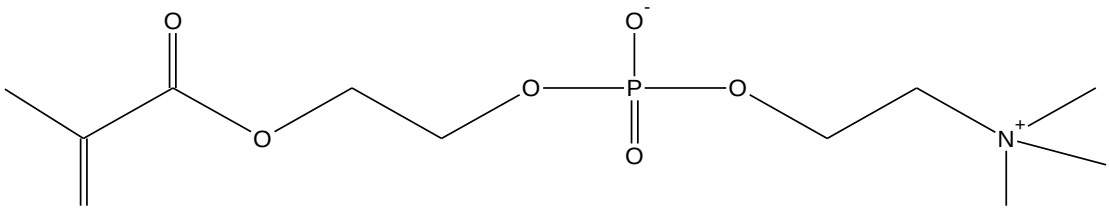

Figure 1.4: Structure of 2- Methacryloyloxyethyl Phosphorylcholine

Random copolymers of MPC and n-butyl methacrylate (BMA) have been synthesized by free radical copolymerization. [7] However, more effort is being focused towards living radical polymerization to obtain more control over molecular weight and molecular weight distribution. The homopolymerization of MPC via atom transfer radical polymerization (ATRP) was reported along with relatively narrow molecular weight distributions (M_w/M_n = 1.15-1.35) at 20°C. [8] A major drawback associated with ATRP is that there is a metal catalyst which would not be ideal for polymers being used for biomedical applications. Therefore, a living polymerization technique which requires no metal catalyst such as RAFT would be a better alternative. Well defined poly(MPC) was prepared by RAFT polymerization at 70°C in water. Their molecular weight distribution was relatively narrow (M_w/M_n = 1.26), but on the other hand molecular weights reported by GPC showed deviation from the theoretical average molecular weight. [9]

Phosphorylcholines are an important component of the cell membrane and consequently when phosphorylcholine based polymers are used as surface coatings they are highly

resistant to protein adsorption and cellular adhesion. [10-15]. Ishihara's group has suggested that the biocompatibility of poly(MPC) is related to its hydrophilic nature based on differential scanning calorimetry studies. [16] These findings have promoted the development of various biomedical devices and implants with improved biocompatibility.

Poly(MPC) has potential for many applications in the biomedical field due its excellent blood compatibility as shown by Ishihara and Iwasaki. Poly(MPC) was prepared by radical polymerization and evaluated for thrombus formation and interaction between plasma proteins. The results indicated reduced thrombogenicity through an increased coagulation time for polymers copolymerized with poly(MPC) as well as reduced plasma protein adsorption. [17]

Poly(MPC) has been applied as a coating to many different applications to reduce protein adsorption and cell adhesion to medical implants. Choi and Ishihara improved the biocompatibility of titanium alloy by fabricating a multilayered hydrogel composed of poly(MPC) on a titanium substrate. Using a scanning electron microscope (SEM) it was shown that the L929 cells which adhered to titanium coated with poly(MPC) copolymers were significantly lower than those with just titanium alone. This result revealed that the poly(MPC) hydrogel coating was found to inhibit cell attachment, entrap bioactive reagents and control diffusivity. [18] The treatment of restenosis by stent based drug delivery has promoted an interest in haemocompatible coatings that could be used as drug delivery coatings. Studies have shown that phosphorylcholine coatings on different types of stents are biocompatible and do not compound an inflammatory response like other coatings. A six month study was done to suggest that the phosphorylcholine shows longevity in the treatment of restenosis and furthermore may also be coupled with drug

delivery. [19] Palmer and Lewis evaluated the drug delivery application of phospholipids by modifying them with cationic polymers which have shown to absorb and adsorb many different drug compounds and release them. As the amount of cationic component was increased there was no evidence of increased protein binding and SEM confirmed that the haemocompatibility was not compromised. Ex vivo and in vivo studies also showed that the cationic polymer was also able to load and release therapeutic DNA fragments that can be used to treat restenosis. [20]

1.4 Polymer Architecture

1.4.1 Dendrimers

In the 1980s a highly branched three dimensional class of macromolecules was born and became one of the most interesting and captivating areas of polymer science and engineering. Dendritic architecture is known as the fourth class of polymer architecture. Up until now there are eight subclasses of dendrimers: (i) dendrimers and dendrons, (ii) linear-dendritic hybrids, (iii) dendronized polymers, (iv) dendrigrafts, (v) hyperbranched polymers, (vi) hyperbranched polymer brushes, (vii) hyperbranched polymer-grafted linear macromolecules and (vii) hypergrafts.[21]

Dendrimers are known as star like shaped polymers which have a sphere like structure and exhibit some unique properties such as increased solubility which distinguish them from linear polymers. Their preparation requires an organized scheme consisting of

synthesis, purification, protection and deprotection steps which limit their production on a large scale. [21]

1.4.2 Hyperbranched Polymers

An alternative to dendrimers that are low in cost and have similar properties are hyperbranched polymers. Hyperbranched polymers were first discovered by DuPont researchers Kim and Webster in the late 1980s and were prepared by a single-step polycondensation of AB_2- type monomers. They are a subclass of dendrimers with a random cascade-branched structure and have the benefits of increased functionality and enhanced solubility compared to linear polymers and do not show a dependency on viscosity at high molecular weights that dendrimers do. [22]

Hyperbranched polymers are generally comprised of three different unit types: terminal, linear and dendritic [23] which are shown in Figure 1.5.

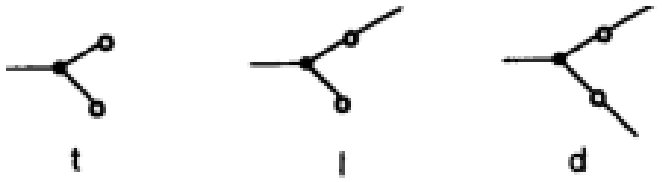

Figure 1.5: Terminal, linear and dendritic units [22]

Figure 1.5 assumes that the units are based on a AB_2 monomer system and the filled circles represent A monomers and the unfilled circles represent B monomers. A terminal unit is when neither B monomer becomes a branch point. Linear units are when only one of the B monomers becomes a branch point and a dendritic unit is when both B monomers become branch points. These units will combine together and form a hyperbranched structure. An example is shown in Figure 1.6.

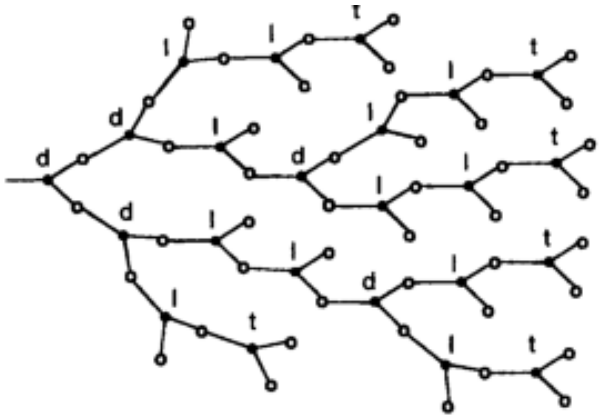

Figure 1.6: Hyperbranched structure with assignment of building units [24]

While RAFT is known for being able to produce polymers with narrow molecular weight distributions, Dong and Li reported the characterization of a hyperbranched styrenic asymmetric divinyl with a broad molecular weight distribution. The hyperbranched vinyl polymers showed a higher molecular weight distribution and a low Mark-Houwink exponent α value compared with their linear counterparts. Figure 1.7 shows the RAFT polymerization mechanism of the asymmetric divinyl monomer. In scheme I the monomer has an allylic group represented by A and a styrenic group represented by B. Since the styrenic group is more reactive, the polymerization occurs to form the main chain (scheme II). Despite their lower reactivities, some of the macro-radicals will react with the allylic groups and thus the polymer will start growing toward the allyl group creating a branched site (scheme III). These branch sites will then progress into a hyperbranched polymer shown in scheme IV. [25]

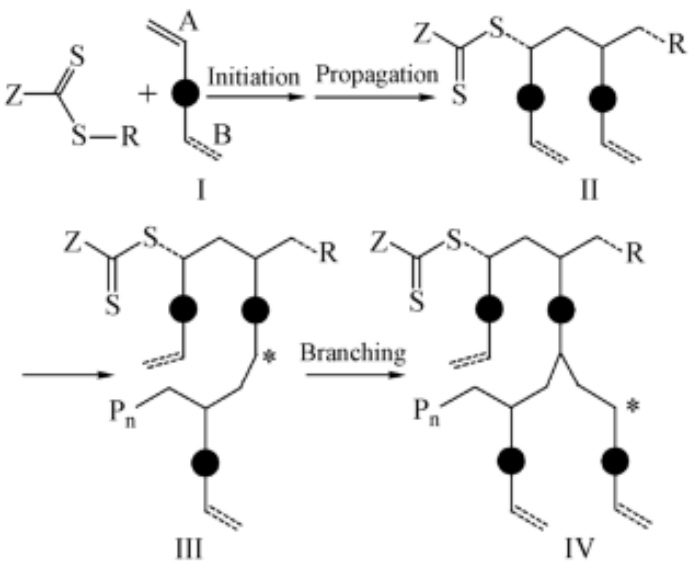

Figure 1.7: Mechanism of RAFT polymerization of an asymmetric divinyl monomer to hyperbranched polymer [25]

Thurecht and Whittaker used RAFT polymerization to synthesize hyperbranched dimethylaminoethylacrylate (DMAEA) using ethyleneglycol dimethylacrylate (EGDMA) as a cross linking agent. The hyperbranched polymers were functionalized by manose via click reactions. The product was synthesized through four distinct steps: the RAFT polymerization of hyperbranched poly(DMAEA-*stat*- tFEA) using EGDMA as a cross linker, the removal of the RAFT end group and the addition of the mannose via click reaction. Molecular weight and distribution was characterized using gel permeation chromatography (GPC). The molecular weight distributions were greater than 1.8. [26]

Hyperbranched glycopolymers were synthesized via RAFT polymerization with the incorporation of *N*,*N*′- Methylenebis(acrylamide) as a cross linking agent by Ahmed and Narain. These polymers were synthesized and characterized by GPC for molecular

weight and distribution and their structures were verified through ^{1}H-NMR. The molecular weight was varied from 24kDa-38 kDa and the molecular weight distributions ranged from 1.74-2.5. [27]

1.5 Applications for gene delivery

Gene therapy is an attractive approach for the treatment of genetic disorder. However, the success of gene therapy is dependent on the effectiveness of the delivery system. Gene delivery is based around the design of a carrier system which transports therapeutic DNA into the nucleus of a cell. Generally these carriers are split into two categories: viral and non-viral carriers. Viruses naturally carry genes into cells and as a result have relatively high transfection efficiencies. However, there are a number of drawbacks to viral carriers and these include induced immunogenicity, and limited DNA carrying ability. Due to these drawbacks non-viral carriers are attracting considerable attention. [22]

In order for carriers to be successful they must overcome a series of barriers to gain access to the membrane surface, cytoplasm and nucleus of the cell to translate genes into proteins. Figure 1.8 shows the barriers to gene delivery [28].

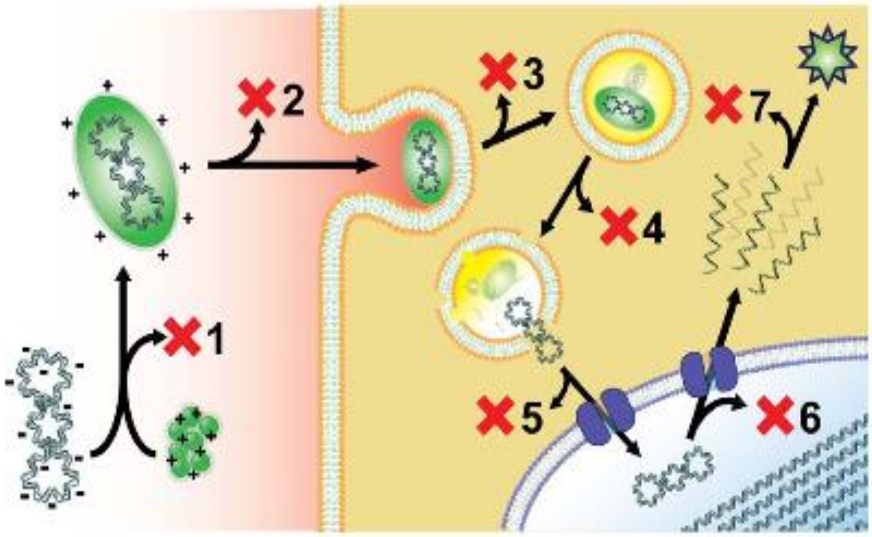

Figure 1.8: Barriers to gene delivery [28]

Before the DNA even approaches the cell it must form a complex with a polymer or else it can be lost before it gets to the cell. **(1)** Once the complex is formed it has the risk of being cleared from circulation by passage through the kidneys or liver, variations in pH, opsonization, proteases and nucleases. **(2)** The complex must bind to the cell and interact with the cell surface by electrostatic interactions, adsorption or ligand receptor binding or else the complexes bound may not be internalized. **(3)** After internalization, the endosome is degraded and as a result a portion of the DNA can be degraded as well. **(4)** After escaping the endosome, the complex must unpack the DNA or else risks preventing it from entering the nucleus. **(5)** Translational efficiencies are a rate limiting obstacle in non viral gene delivery. Some carriers give different levels of expression depending on the type of carrier. **(6,7)** Pollard and Remy have shown that when lipofectamine was compared to the adenovirus, it took a dose that was three thousand times higher for

lipofectamine to give the same level of expression as the adenovirus even though lipofectamine was being uptaken higher on a per carrier basis. [4,28,29]

There are many different entry mechanisms upon which a non-viral carrier may enter the cell however, this review will focus on macropinocytosis clatherin based endocytosis, claveolae based endocytosis which is shown below in Figure 1.9. Cationic polymers can be internalized by macropinocytosis [30], while clathrin and caveolae mediated endocytosis have been shown to be the mechanisms required to uptake lipoplexes and polyplexes. [31]

Cationic polymers bind to heparin sulfate proteoglycans (HSPGs) which are found on the surface of cells and act as receptors. [32] The macropinosomes are fluid filled vesicles and can either fuse with late degradative endosomes or be trafficked directly to the nucleus. [28] **(A)** Clathrin-mediated endocytosis is shown in **B.** Clathrin-coated pits form upon receptor-ligand binding. The formation of these pits is mediated by the adaptor protein AP-2. [33] Dynamin then severs the clathrin-coated pit from the cell membrane and fuses with and forms the clathirin coated vesicle. [34,35] These vesciles can fuse with late acidic endosomes or trafficked to the nucleus directly by microtubules. [28] **C** shows caveolae-mediated endocytosis. Caveolae caves are shown by the plasma membrane and are coated with membrane proteins known as caveolins. [36] The endocytosis proceeds through the oligomerization of caveolin and actin-dependant internalization of caveolae. This results in the formation of caveosomes which can then either fuse with late degradative endosomes or be trafficked to the nucleus through microtubules. [28]

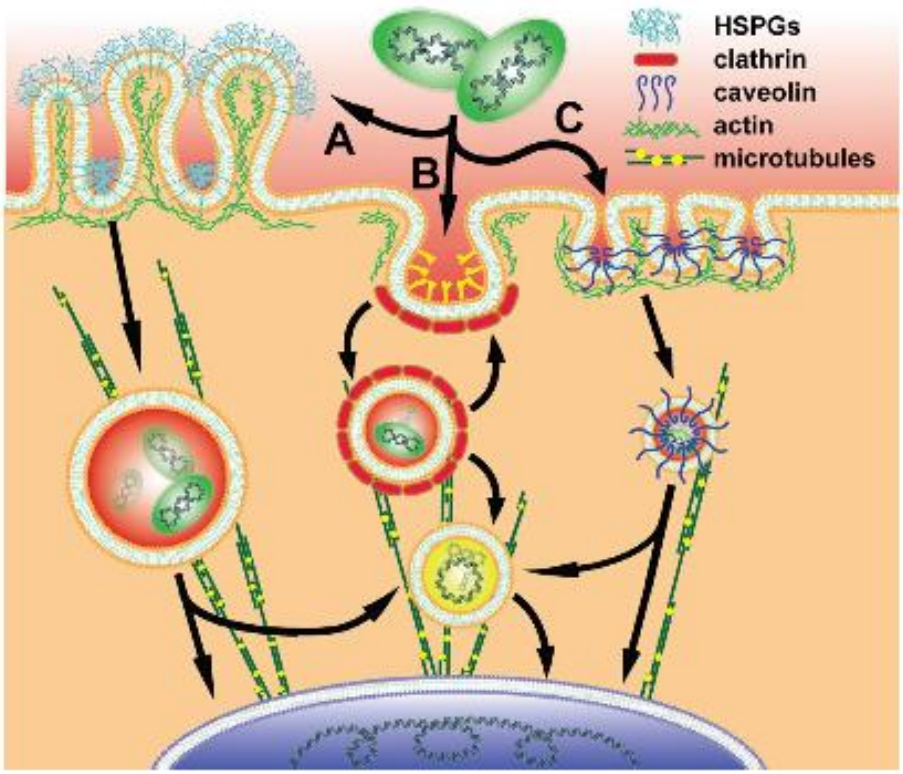

Figure 1.9: Endocytic pathways for non-viral carriers [28]

Ahmed and Narain have reported the synthesis of poly(MPC) copolymers via RAFT polymerization for gene delivery.[37] Cationic poly(MPC) statistical and block copolymers were synthesized and it was found that the statistical copolymers produced large particles and as a result showed poor gene transfection efficiency compared to the block copolymers. In addition to showing enhanced gene expression the block copolymers showed minimum toxicity (with ~60% cell viability). The results of these findings showed that poly(MPC) copolymers would be ideal candidates as potential gene delivery vectors by retaining the antifouling properties of poly(MPC) as well as the enhanced gene expression of the cationic component. [37]

Many studies have evaluated the effect that different molecular weights and compositions have on cell transfection but little attention has been given to polymer architecture. Nakayama has synthesized hyperbranched star vectors by living radical polymerization techniques. Cationic poly(N,N-dimethylaminopropyl acrylamide)(PDMAPAAm)- based star vectors with no branches, 3, 4 or 6 branching numbers. The star vectors formed polyplexes by mixing with DNA and the by increasing the degree of branching the relative gene expression activity of the DNA also increased. Preliminary in vivo studies of blocked star vectors showed high gene expression in the liver, kidneys or spleen when injected into mice. It was concluded that these blocked star vectors may have the potential for clinical use as a non-viral vector. [22]

References

[1] Mishra, V., & Kumar, R. (2012) Living Radical Polymerization- A Review, *Journal of Scientific Research*, 56(13), 141-176.

[2] Balard, H., & Braun, D. (1981). Polymerisationsauslosung mit substituierten Ethanen , 4a) Kinetik der Polymerisation von Methylmethacrylat mit, *32(6)*, 3195-3206.

[3] Moad, G., Chiefari, J., Roshan, T., Mayadunne, A., Moad, Catherine, Moad., Postma, Almar., Razzardo, E., Thang, San., .-vch V. (2002). Initiating Free Radical Polymerization. *Macromolecules Symposium*, 182(1), 65-80.

[4] M. Semsarilar and S. Perrier, (2010). 'Green' reversible addition-fragmentation chain-transfer (RAFT) polymerization**.** *Nature Chem.*, **2(10)**, 811

[5] Braunecker, W. a., & Matyjaszewski, K. (2007). Controlled/living radical polymerization: Features, developments, and perspectives. *Progress in Polymer Science*, *32*(1), 93-146.

[6] Monge, S., Canniccioni, B., Graillot, A., & Robin, J.-J. (2011). Phosphorus-containing polymers: a great opportunity for the biomedical field. *Biomacromolecules*, *12*(6), 1973-82.

[7] Ishihara, K.; Iwasaki, Y.; Nakabayashi, N. (1999). Polymeric lipid nanosphere consisting of water-soluble poly(2-methacryloyloxyethyl phosphorylcholine-co-n-butyl methacrylate). *Polymer Journal*, (31,12), 1231-1236

[8] Ma, Y., Tang, Y., Billingham, N. C., Armes, S. P., Lewis, A. L., Lloyd, A. W., & Salvage, J. P. (2003). Well-Defined Biocompatible Block Copolymers via Atom Transfer Radical Polymerization of 2-Methacryloyloxyethyl Phosphorylcholine in Protic Media. *Macromolecules*, 36(10), 3475-3484.

[9] Yusa, S.-I., Fukuda, K., Yamamoto, T., Ishihara, K., & Morishima, Y. (2005). Synthesis of well-defined amphillic block copolymers having phospholipid polymer sequences as a novel biocompatible polymer micelle reagent. *Biomacromolecules*, *6*(2), 663-70.

[10] Hayward, J. a, & Chapman, D. (1984). Biomembrane surfaces as models for polymer design: the potential for haemocompatibility. *Biomaterials*, *5*(3), 135-42.

[11] Hayward, J. A., Durrani, A. A., Shelton, J., Lee, D. C., & Chapman, D. (1986). Biomembranes as models for polymer surfaces.III Characterization of a phosphorylcholine surface covalently bound to glass. *Biomaterials, 7(2), 126-131*.

[12] Lewis, A. (2000). Phosphorylcholine-based polymers and their use in the prevention of biofouling. *Colloids and surfaces. B, Biointerfaces*, *18*(3-4), 261-275.

[13] Uchida, T., Furuzono, T., Ishihara, K., Nakabayashi, N., & Akashi, M. (2000). Graft Copolymers Having Hydrophobic Backbone and Hydrophilic Branches . XXX . Preparation of Polystyrene- Core Nanospheres Having a Poly (2-methacryloyloxyethyl phosphorylcholine) Corona. *Polymer*, 38(17), 3052-3058.

[14] Clarke, S., Davies, M. C., Roberts, C. J., Tendler, S. J. B., Williams, P. M., Byrne, V. O., Lewis, A. L., et al. (2000). Surface Mobility of 2-Methacryloyloxyethyl Phosphorylcholine-co-Lauryl Methacrylate Polymers. *Langmuir*, 16 (11), 5116-5122.

[15] Murphy, E. F., Lu, J. R., Lewis, A. L., Brewer, J., Russell, J., & Stratford, P. (2000). Characterization of Protein Adsorption at the Phosphorylcholine Incorporated Polymer-Water Interface. *Society*, 33(12), 4545-4554.

[16] Lewis, A. (2000). Phosphorylcholine-based polymers and their use in the prevention of biofouling. *Colloids and surfaces. B, Biointerfaces*, *18*(3-4), 261-275.

[17] Ishihara, K., Iwasaki, Y., & Nakabayashi, N. (1998). Novel biomedical polymers for regulating serious biological reactions. *Materials Science and Engineering: C*, *6*(4), 253-259.

[18] [24] Choi, J., Konno, T., Matsuno, R., Takai, M., & Ishihara, K. (2008). Surface immobilization of biocompatible phospholipid polymer multilayered hydrogel on titanium alloy. *Colloids and surfaces. B, Biointerfaces*, *67*(2), 216-23.

[19] Lewis, a L., Tolhurst, L. a, & Stratford, P. W. (2002). Analysis of a phosphorylcholine-based polymer coating on a coronary stent pre- and post-implantation. *Biomaterials*, *23*(7), 1697-706.

[20] Palmer, R. R., Lewis, A. L., Kirkwood, L. C., Rose, S. F., Lloyd, A. W., Vick, T. a, & Stratford, P. W. (2004). Biological evaluation and drug delivery application of cationically modified phospholipid polymers. *Biomaterials*, *25*(19), 4785-96.

[21] Deyue Yan, C. G. and H. F. (2011). *Hyperbranched Polymers: Synthesis, Properties and Applications* (pp. 1-7). John Wiley & Sons.

[22] Nakayama, Y. (2012). Hyperbranched Polymeric "Star Vectors" for Effective DNA or siRNA Delivery. *Accounts of chemical research*,XXX(XX),XXXX

[23] Maier, G., Zech, C., Voit, B., & Komber, H. (1998). An approach to hyperbranched polymers with a degree of branching of 100%. *Macromolecular Chemistry and Physics*, *199*(12), 2655-2664.

[24] [Frey, H., & Hölter, D. (1999). Degree of branching in hyperbranched polymers. 3 Copolymerization of ABm-monomers with AB and ABn-monomers. *Acta Polymerica*, *50*(2-3), 67-76.

[25] Dong, Z.-min, Liu, X.-hui, & Li, Y.-sheng. (2009). Synthesis and Characterization of Hyperbranched Vinyl Polymers From Raft Polymerization of an Asymmetric Divinyl Monomer. *Chinese Journal of Polymer Science*, *27*(02), 285.

[26] Thurecht KJ, Blakey I, Peng H, Squires O, Hsu S, Alexander C, Whittaker, AK (2010). Functional Hyperbranched Polymers: Toward Targeted *in Vivo* ^{19}F Magnetic Resonance Imaging Using Designed Macromolecules.*J Am Chem Soc*,132(15), 5336–5337.

[27] Ahmed, M., Lai, B. F. L., Kizhakkedathu, J. N., & Narain, R. (2012). Hyperbranched Glycopolymers for Blood Biocompatibility.*Bioconjugate Chem*, 23(5), 1050-1058.

[28] Adler, A. F., & Leong, K. W. (2010). Emerging links between surface nanotechnology and endocytosis: impact on non-viral gene delivery. *Nano today*, *5*(6), 553-569.

[29] Moad, G.; Rizzardo, E.; Thang, S. H. (2005). Living Radical Polymerization by the RAFT Process .*Aust. J. Chem*, 58(6), 379-410

[30] Rejman, J., Bragonzi, A., & Conese, M. (2005). Role of clathrin- and caveolae-mediated endocytosis in gene transfer mediated by lipo- and polyplexes. *Molecular therapy : the journal of the American Society of Gene Therapy*, *12*(3), 468-74.

[31] Khalil, I. a, Kogure, K., Futaki, S., & Harashima, H. (2006). High density of octaarginine stimulates macropinocytosis leading to efficient intracellular trafficking for gene expression. *The Journal of biological chemistry*, *281*(6), 3544-51.

[32] Hess, G. T., Humphries, W. H., Fay, N. C., & Payne, C. K. (2007). Cellular binding, motion, and internalization of synthetic gene delivery polymers. *Biochimica et Biophysica Acta (BBA) - Molecular Cell Research.*, *1773*(10), 1583-1588.

[33] Conner, S. D., & Schmid, S. L. (2003). Regulated portals of entry into the cell. *Nature*, *422*(6927), 37-44.

[34] Medina-Kauwe, L. K., Xie, J., & Hamm-Alvarez, S. (2005). Intracellular trafficking of non-viral vectors. *Gene therapy*, *12*(24), 1734-51.

[35] D. Lechardeur, A.S. Verkman, G.L. Lukacs, (2005). Intracellular routing of plasmid DNA during non-viral gene transfer**.** *Adv. Drug Deliv*. 57(5).755—767.

[36] Pelkmans, L., & Helenius, A. (2003). Insider information: what viruses tell us about endocytosis. *Current Opinion in Cell Biology*, *15*(4), 414-422.

[37] Ahmed, M., Bhuchar, N., Ishihara, K., & Narain, R. (2011). Well-controlled cationic water-soluble phospholipids polymer-DNA nanocomplexes for gene delivery. *Bioconjugate Chemistry*, *22*(6), 1228-38.

2. Instrumentation/Experimental Methods

2.1 Gel Permeation Chromatography (GPC)

Gel permeation chromatography (GPC) or Size Exclusion Chromatography (SEC) is a technique used to determine the molecular weight (M_n) and molecular weight distribution (M_w/M_n) of polymers and proteins. [1]

GPC is understood as the separation of molecules based on their hydrodynamic radius (R_h) or volume (V_h). The molecules are separated through a packed column which contains porous a material such as polystyrene gels, glass beads or silica gel. [1]

Based on their R_h larger molecules are unable to pass through the pores and as a result are eluted faster at the interstitial volume V_i. Smaller molecules elute slower because they have to pass through the pores and therefore will elute at the sum of the interstitial volume and the pore volume (V_i+V_p). Molecules that have a variety of different sizes have some particles that pass through the pores and are eluted at the elution volume V_e shown in equation 2: [2]

$$V_e = V_i + K_{sec} \times V_p \quad (2)$$

Figure 2.1 shows a block diagram of the GPC instrumentation. A continuous mobile phase flows through the system and is first passed through a pump where it is degassed. At the injection valve, which can either be automated or manual, a sample is injected. The sample is carried to the packed bead column where it is separated by size and passed

through detectors that are coupled with the GPC and create a plot of signal to elution time. The most commonly used detectors are: [2, 3, 4]

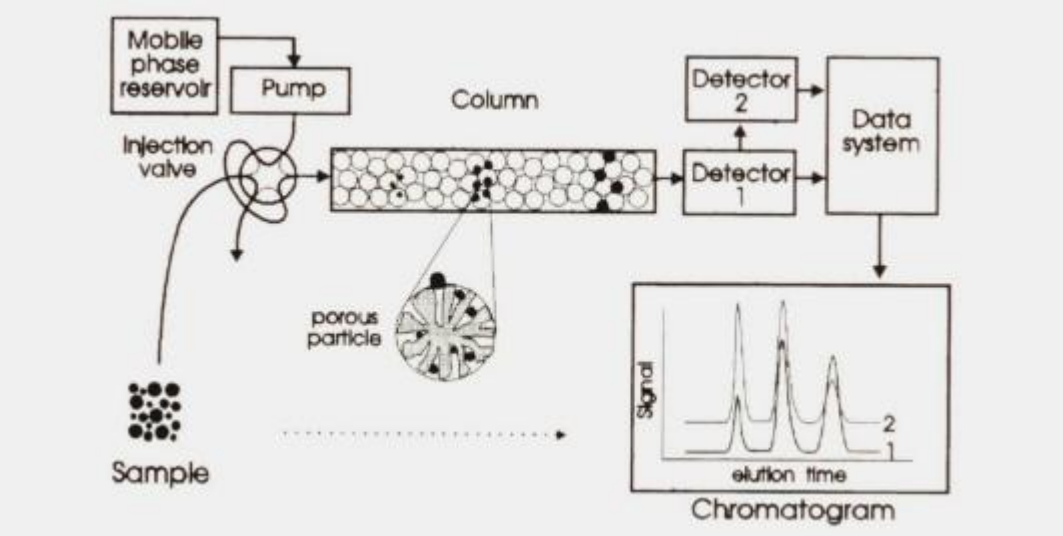

Figure 2.1: Block Diagram of GPC instrumentation [2]

1) Refractive Index Detectors (RI): Measure the deflection of the light beam when the sample enters the sample cell and changes the angle of reflection. These detectors are used to calculate molar mass and concentration profiles.

2) UV /Vis detectors: Different compounds absorb different wavelengths of radiation and UV/Vis detectors typically measure the absorbance of a compound at a fixed wavelength but at relatively low energy levels. Since the majority of organic compounds can be analyzed using UV/Vis they are generally used in protein characterization or copolymer analysis. Like RI, they are used to calculate molar mass and concentration profiles.

3) Light scattering detectors: Determine the molar mass of particles in solution by detecting how they scatter light and give a direct measure of molecular mass. There are many different types of light scattering detectors such as Low Angle Laser Light Scattering (LALLS), Right Angle Laser Light Scattering (RALLS) or Multi Angle Laser Light Scattering (MALLS).

Three different GPC calibration techniques can be used and each employs a unique combination of detectors:

2.1.1 Conventional Calibration

This type of calibration technique is usually coupled with a RI detector or a UV/Vis detector. Retention volume is plotted against the logarithm of the molecular weight (MW) to obtain a calibration curve used to estimate the molecular weight of a sample. [5]

Conventional calibration requires the user to inject a series of polymer standards with known molecular weights and narrow molecular weight distributions. These standards are run through the GPC and the retention volume of the corresponding standard molecular weights is measured. Then after the calibration data has been collected a calibration curve is constructed to fit equation 3: [5]

$$Log\ M = A_o + A_1 V + A_2 V^2 + \cdots + A_n V^n \quad (3)$$

Figure 2.2 shows the molecular weight of each sample and how they are estimated using the calibration curve. The samples are analyzed by finding the corresponding concentration (or weight fraction) from the RI measurement and relating it to the molecular weight in the calibration curve. The i^{th} index corresponds to the i^{th} polymer

chain. These values are collected as data points and then summed across the curve obtained from the RI. [5]

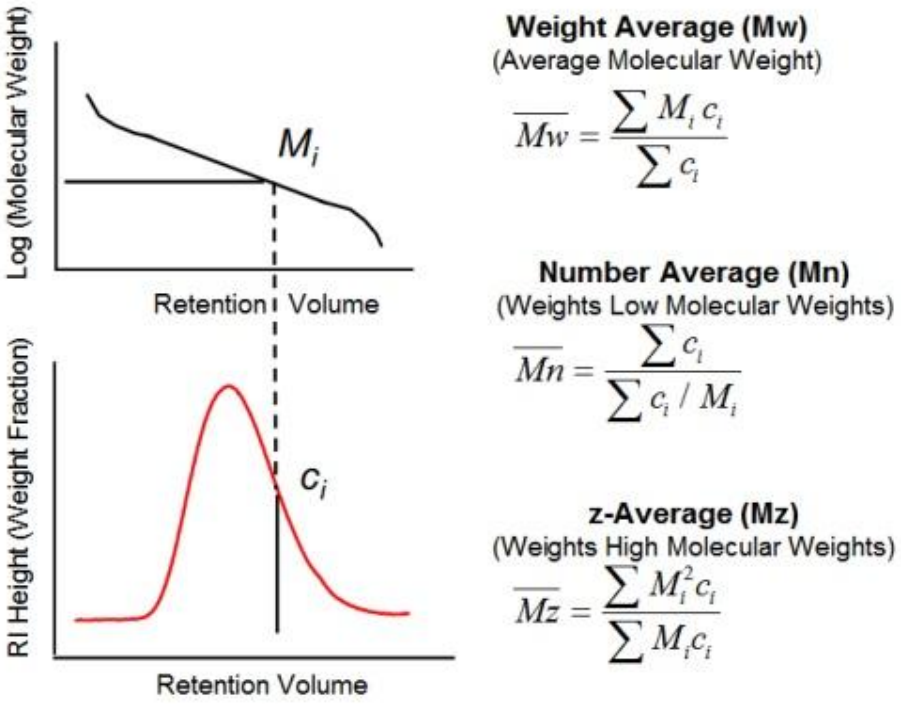

Figure 2.2: Molecular weight calculated by conventional calibration [5]

2.1.2 Universal Calibration

A major assumption in conventional calibration is that the density of the polymer used to obtain the standard should be the same as the sample being tested. Unfortunately, this is rarely the case, and as a result an improved calibration technique that incorporates a viscometer detector can be used.

Conventional calibration forms a relationship with the molecular weight and retention volume of the sample but, when molecules are separated in a column they are separated based on their hydrodynamic radius or volume. Therefore, in order to obtain an improved

calibration curve a relationship between the hydrodynamic volume and retention volume should be obtained. [5] With the use of a viscometer, it is possible to measure the intrinsic viscosity (IV) which is related to the molecular weight (MW) and hydrodynamic volume (V_h) through equation 4:

$$M_w \times IV = \frac{5}{2} \times N_A \times V_{\square} \quad (4)$$

In universal calibration, Log (MW*IV) versus retention volume is used as a calibration curve instead of molecular weight versus retention volume. The same equations described in conventional calibration are used to determine number average molecular weight, M_n and weight average molecular weight, M_w. Figure 2.3 shows how a universal calibration curve is used to calculate sample molecular weight. [5]

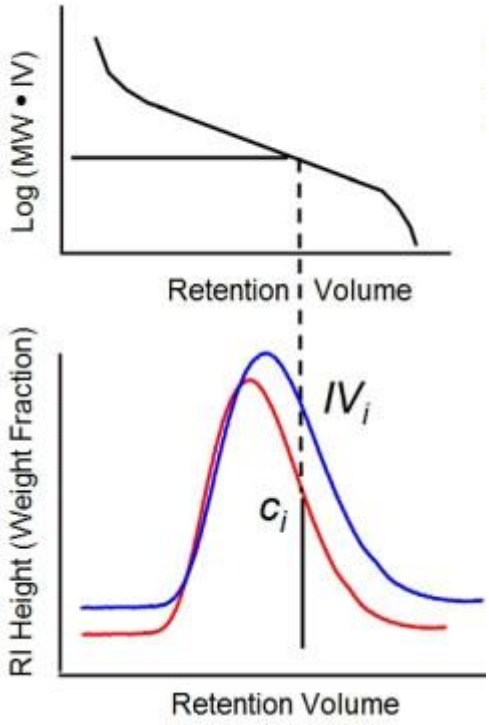

Figure 2.3: Universal calibration method [5]

By calibrating the curve using hydrodynamic volume to retention volume, the user is able to obtain true molecular weight distributions and can also provide information about structural properties such as branching. [5]

2.1.3 Triple Detection Calibration

This calibration technique is the most accurate method because it incorporates three different detectors working together (RI (or UV/Vis), viscometer and light scattering detector). The RI or UV/Vis detector measures the concentration of the sample, the viscometer measures intrinsic viscosity directly and a light scattering detector measures molecular weight directly. Consequently, this eliminates the need for any column calibration except for running a single narrow standard. [5]

M_w and M_n are calculated using the following equations:

$$M_w \propto \frac{LALS\ Peak\ area}{RI\ Peak\ area} \quad (5)$$

$$M_n \propto \frac{RI\ Peak\ area}{Molar\ Conc.Peak\ Area} \quad (6)$$

2.2 Nuclear Magnetic Resonance (NMR)

2.2.1 Basis of NMR

Nuclear Magnetic Resonance (NMR) is a technique used in research to determine the content, purity and molecular structure of a compound. NMR is based around the theory that every nuclei of a molecule has a spin and is charged electrically. As a result, this spin and charge gives each molecule a small magnetic field of its own. [6]

When there is no external magnetic field being applied to a molecule the nucleus spins in a random orientation. But as soon as an external magnetic field is applied to this molecule the nucleus will either spin in a direction against the external magnetic field or align with the external magnetic field.

At a specific frequency also known as the resonant frequency, the molecules that spin at a higher energy create a magnetic moment in a direction against the external magnetic field this results in those molecules being at a higher energy state which is also known as the β-state. Conversely, the molecules that spin at a lower energy create a magnetic moment in the direction that aligns with the external magnetic which results in that nuclei having a lower energy state which is known as the α-state. This change in energy is

measured and the results are plotted on a spectrum. Figure 2.4 shows a schematic representation of this phenomenon for the ½- spin nucleus. [6,7]

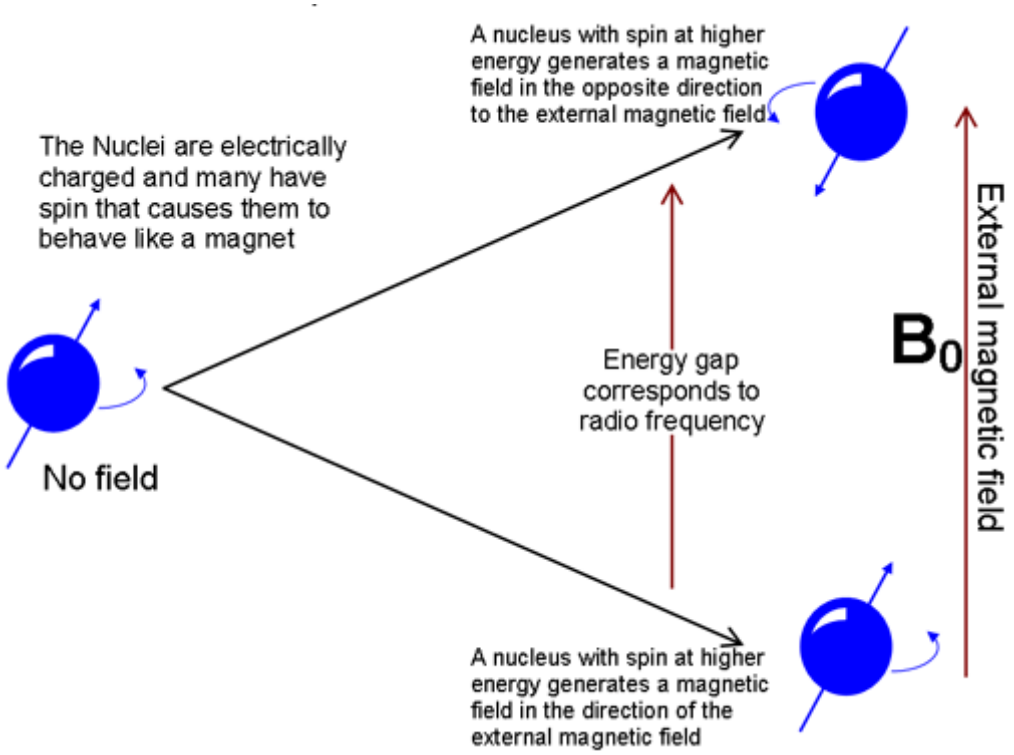

Figure 2.4: Energy levels for the case of spin-1/2 nuclei [7]

2.2.2 Application to Chemistry

All molecules have their own magnetic field. An NMR spectrometer applies an external magnetic field to a molecule and results in an energy separation between the two spin states. The frequency of the magnetic field required to induce this energy separation is known as resonance frequency. Magnetic moment given off by each molecule is known as magnetic shielding and the higher the shielding the higher the resonance frequency required to overcome the shielding. Therefore a concept known as chemical shift is used to characterize different molecules. [8] Figure 2.5 shows the horizontal axis which is used

to map the chemical shift and applied magnetic field strength increases from left to right. Tetramethylsilane (TMS) is used as a zero reference point because it has the highest magnetic shielding and every compound measured will be downfield of TMS. [8]

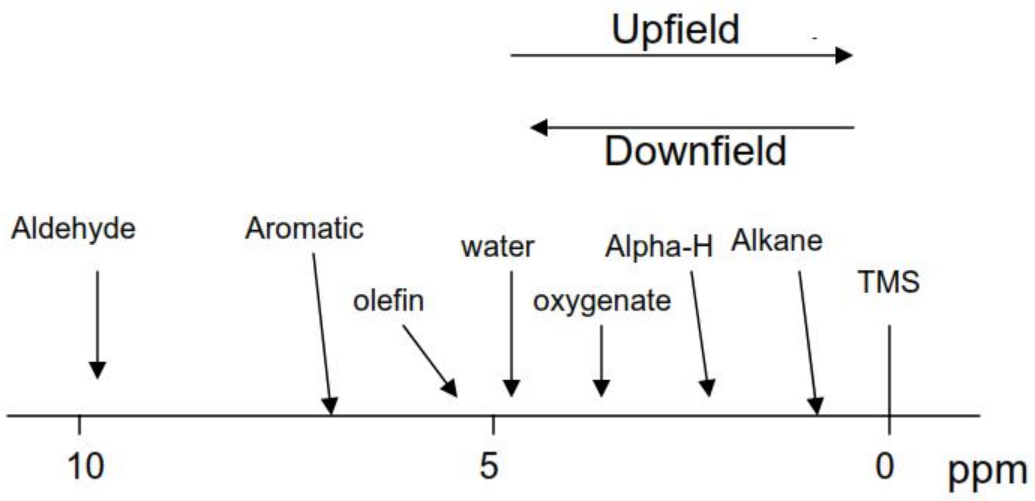

Figure 2.5: Chemical shift of various compounds with reference to TMS [8]

When an unknown sample is measured, to identify properties regarding structure a library of NMR spectra is available and can be used to compare unknown samples with ones that are known. Molar composition of copolymers can be calculated from NMR spectra with equation 7:

$$X_1 n + Y_1 m = A \tag{7a}$$

$$X_2 n + Y_2 m = B \tag{7b}$$

X_1 and Y_1 corresponds to the number of expected protons on the polymer backbone for the first and second monomer respectively. X_2 and Y_2 correspond to the number of expected protons on the polymer branches for each corresponding monomer respectively.

A and B correspond to the total number of protons calculated by NMR for the polymer backbone and branches respectively. Solving the two equations for n and m gives the molar composition of each monomer respectively.

2.3 Gel electrophoresis

Agarose Gel electrophoresis is the most common way of separating DNA. DNA molecules are separated based on charge by applying an electric field to an electrophoretic apparatus. The voltage applied is proportional to the migration rate of DNA fragments and as the voltage increases the migration rate increases. The DNA is detected by the addition of ethidium bromide which is an intercalating agent that places itself between two adjacent pairs of DNA. Therefore, when the gel is exposed to fluorescence it can be seen under a transluminator. The gel is run in a buffer solution which provides ions to support electrical conductivity. The most commonly used buffers are Tris-acetate-EDTA (TAE) and Tris-borate-EDTA (TBE). [9] Figure 2.6 shows a typical gel electrophoresis process.

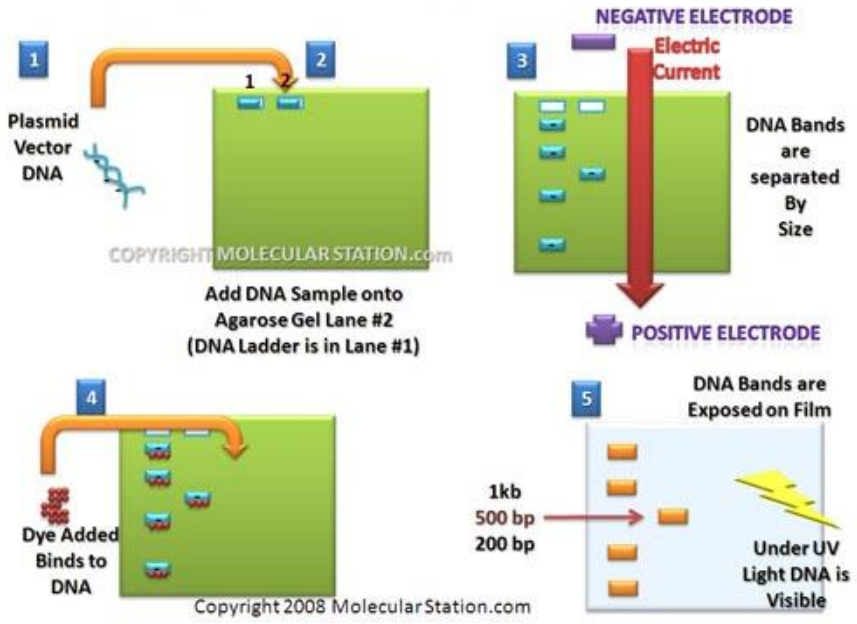

Figure 2.6: Agarose Gel Electrophoresis method [10]

2.4 Beta-galactosidase Assay

Beta-galactosidase (β-gal) is an enzyme used in cells to cleave lactose into a molecule of glucose and galactose. However when used as a assay, instead of lactose the β-gal cleaves ortho-Nitrophenyl-β-galactosidase (ONPG) into galactose and ONP. Then ONP gives off a yellow color and can absorb 420nm of light. As the intensity of the light increases, so does the β-gal activity. The mechanism is shown below in Figure 2.7. [11]

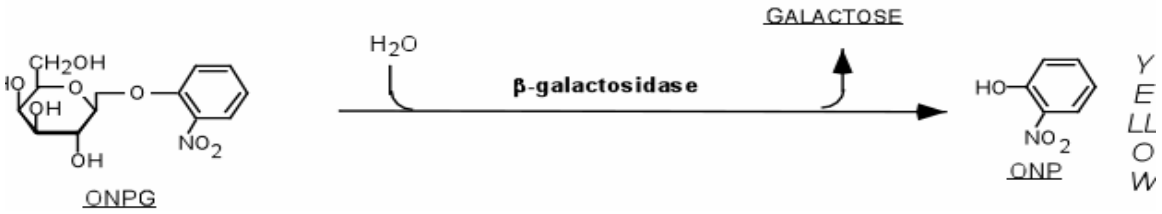

Figure 2.7: ONPG cleaved by β-galactosidase into galactose and ONP [11]

B-mercaptoethanol (BME) is also added to the reaction buffer to stabilize the β-gal enzyme. The thiol group on the BME is responsible for reacting with oxygen in the air and oxidizing (inactivating) over time. [11]

Enzyme activity is calculated from the equation (8) proposed by (Miller, 1972)

$$Miller\ Units = 1000 \times \frac{(OD_{420} - 1.75 \times OD_{550})}{(T \times V \times OD_{600})} \quad (8)$$

Our lab uses a modified form of the Miller equation (9) which is shown below.

$$U/mL = 1000 \times \frac{(OD_{420} - OD_{550}) \times 4.5 \times V_t}{(T \times V_C)} \quad (9)$$

2.5 Bicinchoninic Acid assay

The bicinchoninic acid (BCA) assay depends on a reaction known as the Biuret reaction. Any peptides containing three or more amino acid residues will complex with cupric ions (Cu^{2+}) and the Biuret reaction reduces them from $Cu^{2+}$to Cu^{+} (cuprous ions) in an alkaline environment. This reaction is step one in the BCA assay and is shown in Figure 2.8. [12]

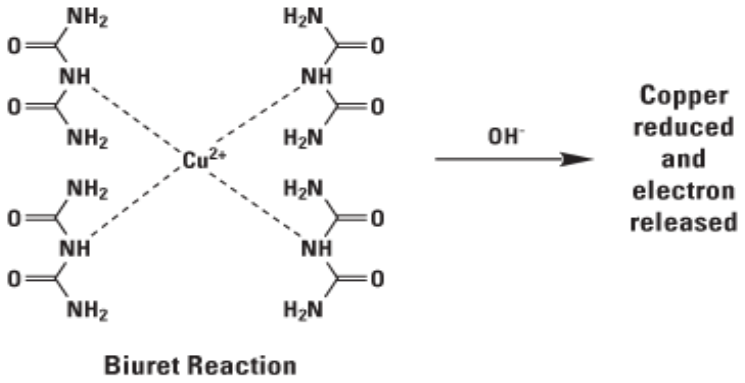

Figure 2.8: Protein induced Biuret reaction [12]

The BCA assay combines the Biuret assay with the detection of the cuprous cation (Cu^{+}) by bicinchoninic acid. Figure 2.9 shows the chelation of BCA with the cuprous cation. The chelation results in an intense purple color which can be measured at wavelengths between 550 – 570 nm. [12]

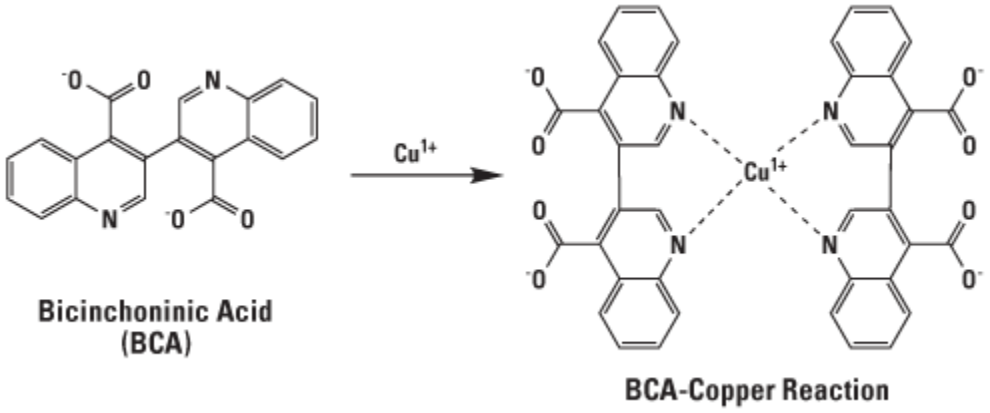

Figure 2.9: Chelation of BCA with the cuprous ion [12]

The samples are prepared in wells and then the absorbance or transmittance (intensity of purple color) is measured with a spectrophotometer. Figure 2.10 shows a standard curve for bovine serum albumin (BSA), which relates the net absorbance to the protein concentration (µg/mL). [12] After knowing the protein concentration we can calculate the percent activity of β-gal by dividing the enzymatic activity of β-gal per milliliter by the protein concentration and we obtain U (enzymatic activity) / mg (total amount of protein) which is what is referred to as transfection efficiency.

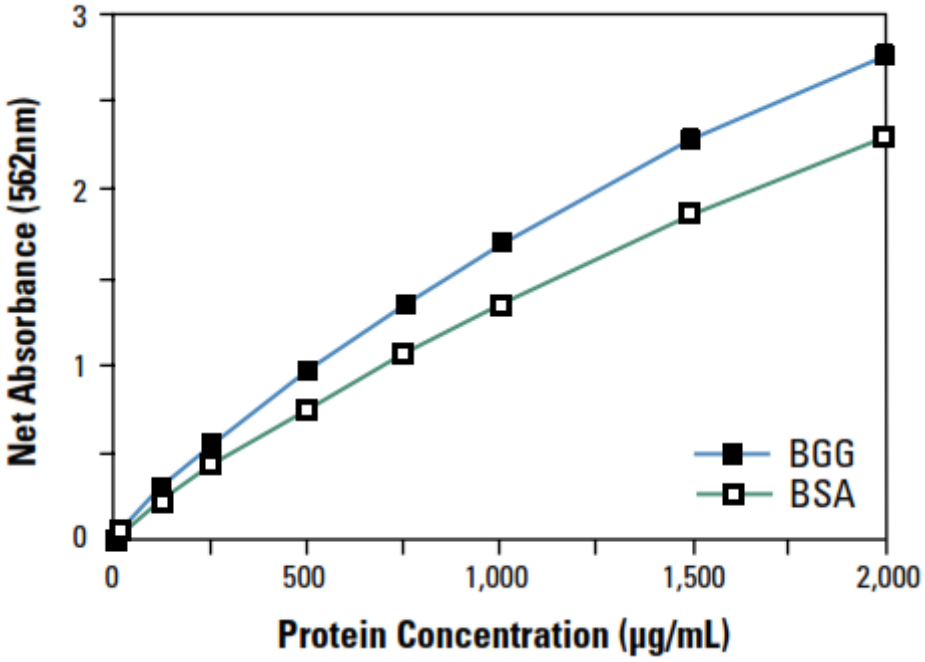

Figure 2.10: Typical standard BCA curve [12]

2.6 Materials

MPC with 7.0 ppm inhibitor was obtained from NOF.co (Tokyo, Japan) [9]. 2-Aminoethyl methacrylamide hydrochloride (AEMA) and Cyanopentanoic acid dithiobenzoate (CTP) were synthesized according to previous reports [10-12]. 4,4'-Azobis (4-cyanovaleric acid) (ACVA) and Ethyleneglycol Dimethacrylate (EGDMA) was purchased from Sigma Aldrich. *N,N'*-Methylene-bis-acrylamide (MBAm) was purchased from Bio-Rad Laboratories (Hercules, CA) and the 2,2-Dimethacroyloxy-1-ethoxypropane (DEP) cross linker was synthesized in the lab. The structures of the monomers are shown below.

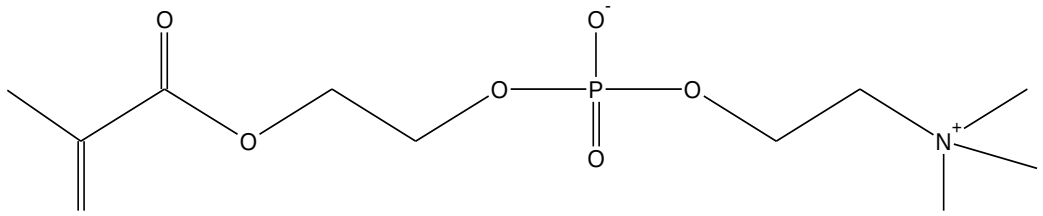

2- methacryloyloxyethyl phosphorylcholine (MPC)

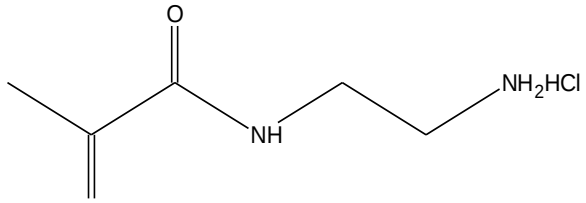

2- aminoethyl methacrylamide hydrochloride (AEMA)

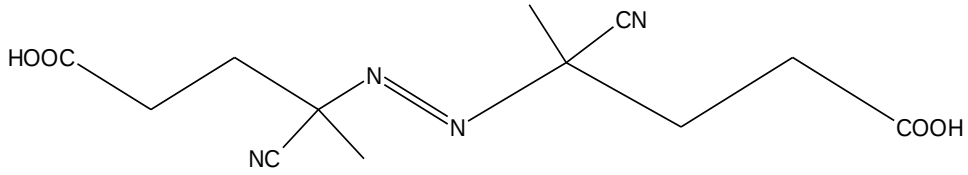

4,4'-azobis(4-cyanovaleric acid) (ACVA)

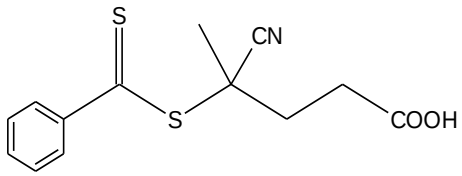

4-cyanopentanoic acid dithiobenzoate (CTP)

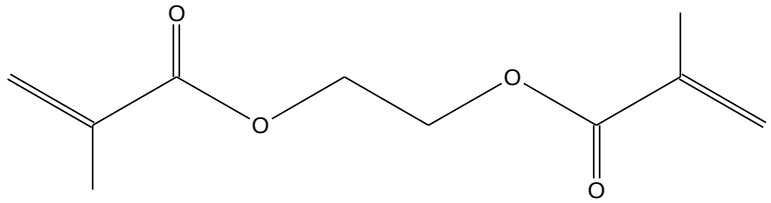

Ethyleneglycol Dimethacrylate (EGDMA)

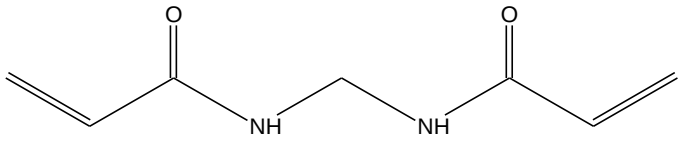

N,N'-Methylene-bis-acrylamide (MBAm)

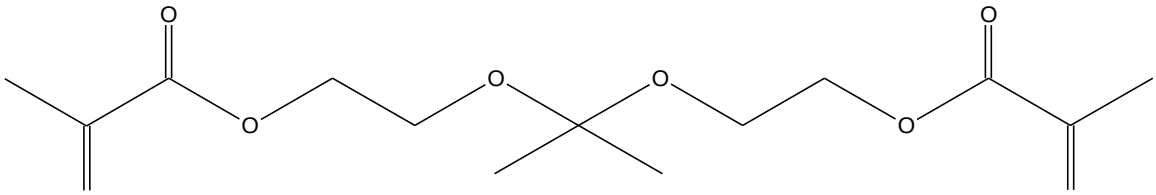

2,2-Dimethacroyloxy-1-ethoxypropane (DEP)

Figure 2.11: Structures of monomers, initiator, chain transfer agent and cross linkers

Branched PEI (Mw= 25kDa), O-Nitrophenyl b-D-galactopyranoside, (ONPG) (enzymatic), β –Mercaptoethanol, 3-[(3-Cholamidopropyl) dimethylammonio]-1-propanesulfonate (CHAPS) were all purchased from Sigma Aldrich. Cell culture media Dulbecco's Modified Eagle Medium (DMEM; high and low glucose with L-glutamine and sodium pyruvate), penicillin (10,000 U/mL), 0.25% trypsin, Dulbecco's modified Phosphate Buffer Saline

(DPBS) and Fetal Bovine Serum (FBS) were purchased from Invitrogen. The Micro BCA assay kit was obtained from Fisher Scientific. Gwiz b-galactosidase plasmid was purchased from Aldevron and bovine serum albumin (BSA) from Promega Corporation.

2.7 Methods

M_n and (M_w/M_n) were both determined at a flow rate of 1.0 mL/min using a Viscotek conventional GPC system equipped with two Waters Ultrahydrogel linear WATO11545 columns (pore size: blend, exclusion limit = 7×10^6) and a viscotek model 250 dual detector. 0.5M sodium acetate/ 0.5M acetic acid buffer was used as an eluent. The GPC was calibrated by six near monodisperse polyethylene oxide standards (M_p – 1.01×10^3-1.01×10^5 g mol^{-1}). The polymers were freeze dried using a Labconco Freezone 2.5. ^{1}H-NMR spectrum was recorded on a Varian 400 or 500 MHz instrument.

2.7.1 Homopolymerization of Hyperbranched poly(MPC)

The homopolymerization of hyperbranched poly(MPC) was conducted via RAFT at 60°C. ACVA and CTP were used as the initiator and CTA respectively. Inside a 10mL schlenck tube MPC (0.5 g, 1.69 mmol), CTP (0.0027 g, 9×10^{-3} mmol, target DP_n=175), ACVA (0.00054 g, 1.9×10^{-3} mmol) and MBAm (0.013 g, 8.4×10^{-2} mmol) were all dissolved in 1.5mL of methanol. The solution was degassed using N_2 for 30 minutes and placed in an oil bath at 60°C for 15 hours. The reaction was quenched using liquid nitrogen. The polymer was precipitated in a large amount of acetone and the M_n and (M_w/M_n) were obtained from aqueous GPC after the polymer was freeze dried overnight.

2.7.2 Copolymerization of Hyperbranched poly(MPC-*stat*-AEMA)

The synthesis was carried out using a similar procedure to the one mentioned above. In a typical procedure: MPC (0.2 g, 0.68 mmol), AEMA (0.1 g, 0.67 mmol) CTP (0.0037 g, 13×10^{-3} mmol, target DP_n=100), ACVA (0.00075 g, 2.7×10^{-3} mmol) and *N*,*N*'-Methylene-bis-acrylamide (0.010 g, 6.8×10^{-2} mmol) were dissolved in 1.5 mL of water

and 0.5 mL of 2-propanol. The solution was degassed using N_2 for 30 minutes and placed in an oil bath at 70°C for 15 hours. The reaction was quenched using liquid nitrogen. The polymer was precipitated in a large amount of acetone, dialyzed against 1L of water over three days to remove any impurities, and then freeze dried overnight. The M_n and (M_w/M_n) were obtained from aqueous GPC and conversion was calculated from ^{1}H-NMR.

2.7.3 Formation of polyplexes

Polyplexes were formed by combining various mass ratios of polymers with 1 mg/mL of β-galactosidase plasmid in OMEM. The complexes were vortexed gently and left at room temperature for 30 minutes before their analysis.

2.7.4 Agarose Gel Electrophoresis

Polyplexes were loaded in 0.7g of agarose with 70 µL of ethidium bromide. The gel was run at 138V for 30 minutes. The DNA bands were visualized using a UV transilluminator (Alpha Innotech, San Leandro, CA) [13]

2.7.5 Cell Culturing

Hep G2 cells were maintained in DMEM which was supplemented with 10% Fetal Bovine Serum (FBS) and 1% penicillin/streptomycin solution in a humidified atmosphere of 5% CO_2 at 37°C. The cells were trypsinized with 0.25% trypsin upon 80% confluency and were seeded in tissue culture plates. [14]

2.7.6 Transfection

In a typical experiment, Hep G2 cells were seeded at a density of 50 000- 100 000 cells per well in a 24 well tissue culture plate and left overnight to grow. The next day the media is removed and 200-400 µL of serum free OMEM is added to each well. The polyplexes are added and the cells are incubated for 4 hours. After 4 hours, the polyplex containing media is removed and replaced with serum containing media and the cells are allowed to grow for 48 hours. The cells then undergo lysis (CHAPS in sodium phosphate lysis buffer) followed by a freeze thaw cycle. [14]

β-galactosidase activity was measured using a β-gal assay. In a 96 well plate 150 µL of 4mg/mL ONPG solution is added to the supernatant lysis volume along with 4.5 µL of a 0.64 µL β-mercaptol-ethanol in 200 µL of 0.1M $MgCl_2$ solution. The plate was incubated at 37°C and the yellow color was detected after 4 hours using a TEGAN Genois Pro microplate reader at 420 nm. Protein content was measured using a BCA assay (Pierce) after 2 hours at 570 nm. [14]

References

[1] Viscotek Setting the Standard for GPC. (2006).*Complete Guide for GPC/SEC/GFC Instrumentation and Detection Technologies*. Retrieved from http://www.particular.ie/info for download/General introduction to GPC and what Viscotek offer.pdf

[2] Mallon, P. P. (2011). Gel Permeation Chromatography (GPC). Retrieved from http://academic.sun.ac.za/polymer/gpectref.htm#general

[3] McNair, Y. K. and H. (2007). *HPLC for Pharmaceutical Scientists*.

[4] Alliance Protein Laboratories. (2011).*Laser Light Scattering*. Retrieved from http://www.ap-lab.com/light_scattering.htm

[5] Understanding GPC/SEC. (2012) Retrieved from http://www.malvern.com/labeng/technology/gel_permeation_chromatography_theory/gpc_sec_theory.htm

[6] Kawulka, K. E. (2008). H NMR and C NMR Spectroscopy. *Chemistry 361/363 Spectroscopy* (pp. 19-23).

[7] Uses of NMR spectroscopy, R. Hoffman, Y. Ozery, (2009) Retrieved fr http://chem.ch.huji.ac.il/nmr/whatisnmr/whatisnmr.html

[8] Edwards, B. J. C., & Ph, D. (1946). Principles of NMR. *Energy*.

[9] Tom Maniatis, E.F. Fritsch, J. S. (1982). Molecular Cloning a laboratory manual. *Principles of Gene Manipulation*, *7*.

[10] Agarose Gel Electrophoresis. (2005) Retrieved from http://www.molecularstation.com/agarose-gel-electrophoresis/

[11] Miller, J. H. (1972). *Experiments in Molecular Genetics* (pp. 352-355).

[12] Thermo Scientific Pierce Protein Assay Technical Handbook Version 2 Table of Contents.

[13] Ahmed, M., Bhuchar, N., Ishihara, K., & Narain, R. (2011). Well-controlled cationic water-soluble phospholipid polymer-DNA nanocomplexes for gene delivery. *Bioconjugate chemistry*, *22*(6), 1228-38.

[14] Ahmed, M., & Narain, R. (2011). The effect of polymer architecture, composition, and molecular weight on the properties of glycopolymer-based non-viral gene delivery systems. *Biomaterials*, *32*(22), 5279-5290.

3. Results and Discussion

RAFT polymerization was used to synthesize poly(MPC) homopolymers and poly(MPC-*stat*-AEMA) copolymers. This polymerization technique provides remarkable control over molecular weight and molecular weight distribution. [1] With the incorporation of a cross-linker, the synthesis of phosphorylcholine and cationic phosphorylcholine hyperbranched polymers were achieved via RAFT polymerization. Three different cross-linkers were used in this study: *N*,*N*'-Methylene-bis-acrylamide (MBAm), Ethylene glycoldimethacrylate (EGDMA) and 2,2-Dimethacroyloxy-1-ethoxypropane (DEP). The molecular weight of the polymers was characterized through GPC and the structures and molar compositions were verified by ^{1}H-NMR.

CTP was used as a chain transfer agent because it was compatible with a wide variety of monomers [3] and shown to control molecular weight distribution through RAFT polymerization of MPC and 2-Lactobionamidoethyl Methacrylamide (LAEMA). [3, 4] The ratio of chain transfer agent to initiator may affect the control over polymerization because if the amount of CTA is fixed, less initiator can result in the reduction of termination reaction. On the other hand, using less initiator can also slow down the rate of the polymerization. [3] In this study, a CTA to initiator ratio of 5:1 was used. Various types of cross-linkers including MBAm, EGDMA and DEP have been used as to synthesize branched structures. [2,5,6,7]. In living radical polymerization, the concentration of cross-linker can significantly affect the topology of the resulting polymers. [8]

3.1 Effect of cross linking agents on molecular weight distribution of poly(MPC)

Table 3.1 shows the effect of a cross linking agent on the molecular weight distribution of poly(MPC).

Table 3.1: Effect of cross linker presence on molecular weight distribution

Name	Polymer	M_n	M_w/M_n	Cross Linker
E1	Poly(MPC)$_{14}$	4138	2.1	MBAm
E30	Poly(MPC)$_{11}$	3487	1.1	None

An M_w/M_n of 1 is used to represent uniform chain length, therefore if a molecular weight distribution deviates from 1, this indicates that not all chains are of equal length and if greater than 1.5 the molecular weight distribution would be characterized as broad.[2,5,6,8,9] The data shows that the incorporation of a cross linking agent resulted in broad molecular weight distributions. Broad molecular weight distributions can be used to characterize hyperbranched molecular structure. [2,5,6,8,9] The broad molecular weight distribution can be explained by the cross linking agent working as a branch point and launching chain growth in another direction. The cross linking agent would attack the C=S on the CTA, the cross linker now has a reactive C=C group at the end which serves as a branch point and consequently creates two points for the chain to grow: one from the C=C group on the cross linker and the other from the polymer backbone. Figure 3.1 shows a hyperbranched poly(MPC) structure with MBAm as the cross linking agent:

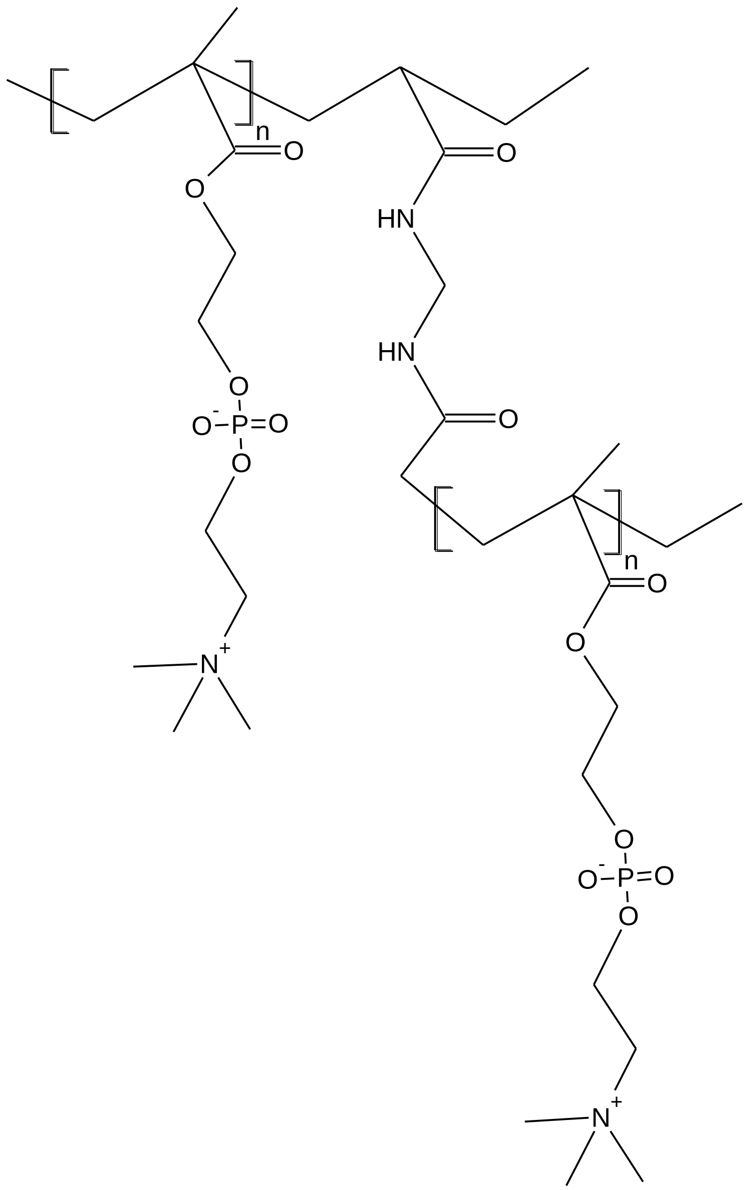

Figure 3.1: Hyperbranched poly(MPC)

Different cross-linkers were used to study the effect of cross-linker size on molecular weight distributions. Table 3.2 shows three different cross-linkers and their corresponding molecular weights, and their effect on molecular weight distribution.

Table 3.2: Comparison of different cross linking agents on molecular weight distribution synthesized via RAFT polymerization

Name	Polymer	Cross-linker	M_n (kDa)	M_w/M_n
E3	Poly(MPC)$_{29}$	MBAm	8777	1.9
E23	Poly(MPC)$_{40}$	EGDMA	12083	1.0
E37	Poly(MPC)$_{13}$	DEP	3903	1.1

The data shows MBAm resulted in broad molecular weight distributions whereas the EGDMA and DEP showed a narrow distribution.

It was difficult to conclude whether or not EGDMA and the DEP cross linker were branch points because hyperbranched polymers can have uniform chain lengths which result in narrow molecular weight distributions. [10]

It was expected that the DEP cross linker may have been a branch point and formed a hyperbranched polymer with narrow molecular weight distribution. To test this hypothesis, two copolymers with different M_n were synthesized using the acid degradable DEP cross linker. [7] Subsequently both polymers were left in a solution of 0.1M HCl

overnight and their M_n was compared before and after exposure to HCl and shown in Table 3.3.

Table 3.3: Degradability of 2,2-Dimethacroyloxy-1-ethoxypropane cross linker in poly(MPC-*stat*-AEMA) copolymer

Name	Polymer	Cross Linker	M_n	M_n (After Hydrolysis)
E8	Poly($MPC_{0.86}$-*stat*-$AEMA_{1.46}$)	DEP	7784	6785
E12	Poly($MPC_{0.91}$-*stat*-$AEMA_{1.17}$)	DEP	9736	10 075

Given that the cross-linker was acid degradable, if it was functioning as a branch point, a decrease in M_n would be expected. The results shows no significant decrease in molecular weight for either polymer which implies that the cross-linker was not functioning as a branch point and furthermore the resulting polymers having a low molecular weight distribution were probably not hyperbranched in structure.

3.2 Analysis of Cationic Phosphorylcholine polymers

MPC and AEMA were copolymerized via RAFT polymerization in the presence of the cross-linker, MBAm. Copolymers were synthesized with different molecular weights and molar ratios. The polymer structures and compositions were determined by NMR spectroscopy (see Figures A1 and A2, Appendix A). The results are shown in Table 3.4.

Table 3.4: Copolymerization of hyperbranched poly(MPC-*stat*-AEMA) via RAFT at different weights and compositions

Name	Target DP_n	Feed Mole ratio	Polymer Mole Composition (NMR)	M_n (Theory) (kDa)	M_n (GPC) (kDa)	M_w/M_n
E10	100	1:1	Poly($MPC_{0.78}$ -*stat*- $AEMA_{1.23}$)	22 950	33 428	2.0
E14	200	1:1	Poly($MPC_{0.60}$ -*stat*- $AEMA_{1.09}$)	45 900	14 100	1.7
E16	50	1:0.5	Poly($MPC_{0.81}$ -*stat*- $AEMA_{1.24}$)	12 468	8129	2.1
E15	100	1:0.5	Poly($MPC_{0.69}$ -*stat*- $AEMA_{1.15}$)	25 133	13 978	5.2
E17	200	1:0.5	Poly($MPC_{0.53}$ -*stat*- $AEMA_{1.29}$)	50 168	11 834	1.9
E18	50	0.5:1	Poly($MPC_{0.84}$ -*stat*- $AEMA_{1.78}$)	10 383	6825	1.7
E19	100	0.5:1	Poly($MPC_{0.77}$ -*stat*- $AEMA_{1.21}$)	20 559	10 721	2.1
E20	200	0.5:1	Poly($MPC_{0.78}$ -*stat*- $AEMA_{1.58}$)	41 282	15 463	2.1

The results showed that M_n values estimated by GPC were significantly lower than the theoretical predicted molecular weight. The subscripts represent the molar composition of each component and were calculated by ^{1}H-NMR. (Figure A3, Appendix A)The results show that, regardless of the feed mole ratio, the content of AEMA residues was larger than MPC. Due to the different structure of hyperbranched polymers, this result may be explained by the difficulty in controlling chain growth due to the presence of a cross linking agent.

Figure 3.2 shows the synthesis of hyperbranched cationic phosphorylcholine copolymers.

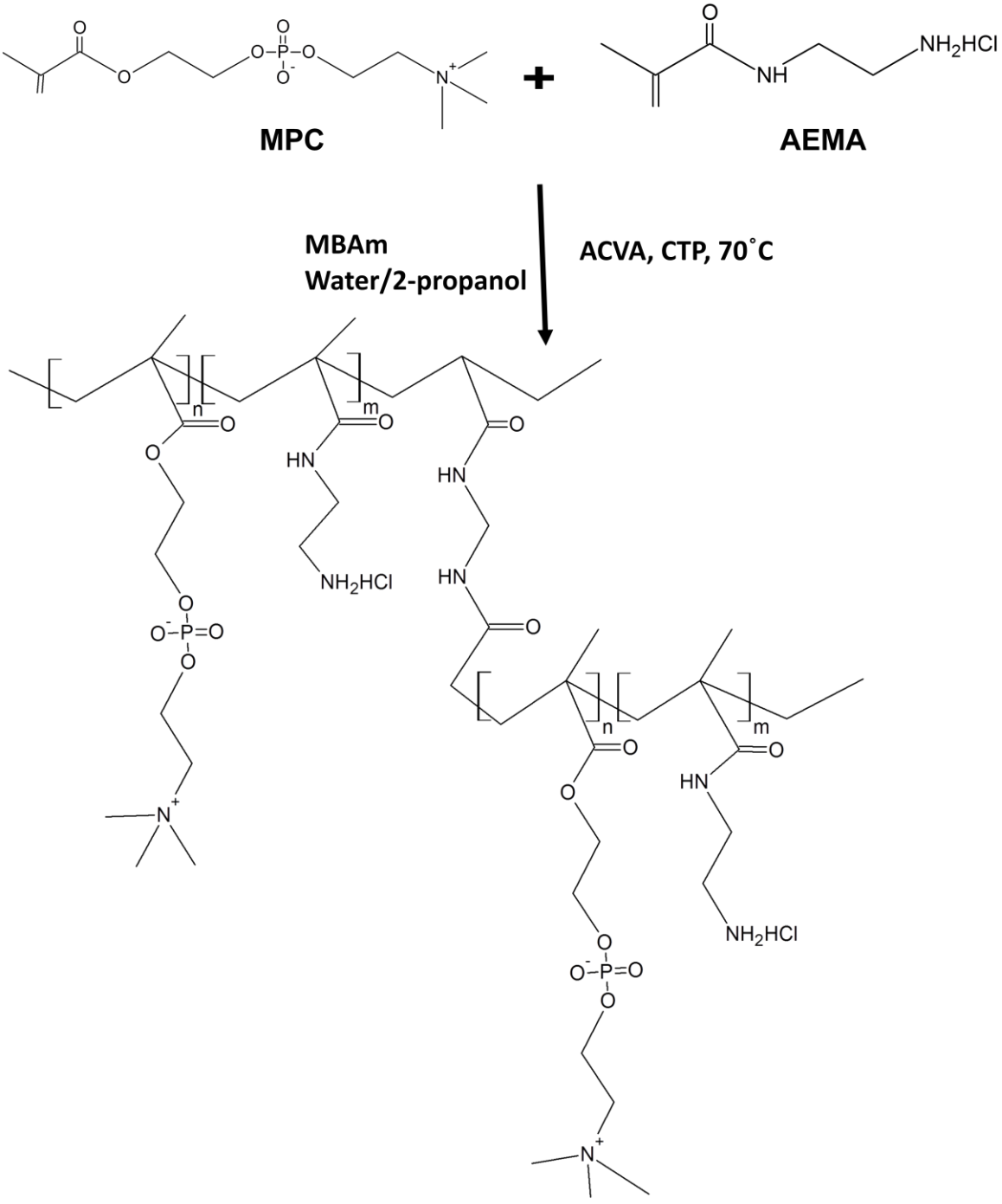

Figure 3.2: Synthesis of hyperbranched poly(MPC-*stat*-AEMA) via the RAFT Process

3.3 Evaluation of Hyperbranched Cationic Phosphorylcholine copolymers as gene carriers

Phosphorylcholine polymers have shown high potential in the biomedical field because of their biocompatibility. [11-14]. MPC is a phosphorylcholine monomer which exhibits enhanced cell viability and gene expression when copolymerized with a cationic monomer and used as a non-viral gene carrier. [15] Various hyperbranched copolymers with MPC and AEMA units were prepared by RAFT polymerization and are listed in Table 3.4 and their chemical structures are shown in Figure 3.2. Previous reports have shown that a high content of cationic component is required to condense DNA and produce stable polyplexes. [16] The polymers were synthesized with varying molecular weights and broad molecular weight distributions and were evaluated for transfection efficiency.

Impurities were removed by dialysis using a membrane MW cut-off of 3600. The purified polymer was characterized by ^{1}H-NMR as shown in Figure A1 (Appendix A).

3.3.1 Agarose Gel Electrophoresis

The copolymers were mixed with Beta galactosidase plasmid DNA and run in an agarose gel to confirm their DNA binding ability. Being a zwitterionic monomer, MPC contains both negative and positive charges in its structure giving it an overall neutral charge. As a result, MPC monomer was copolymerized with a cationic monomer to effectively bind to negatively charged DNA. 1.2µg of DNA was added to each well and was kept consistent and increased amounts of polymer were added to study the affect of polymer/DNA mass ratio on complexation. E14 and E10 which were run on an agarose gel and are shown in

Figure 3.3.

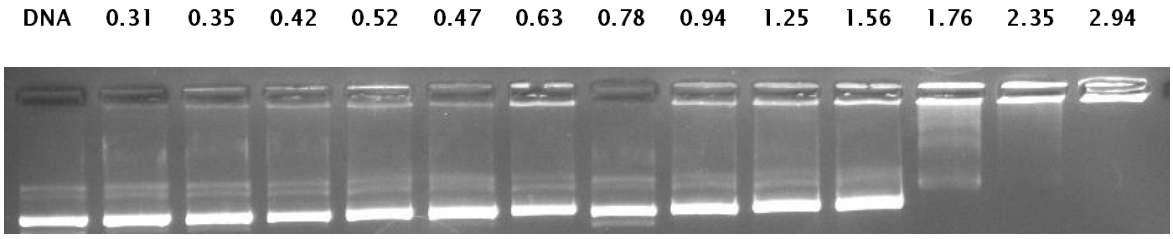

(a)

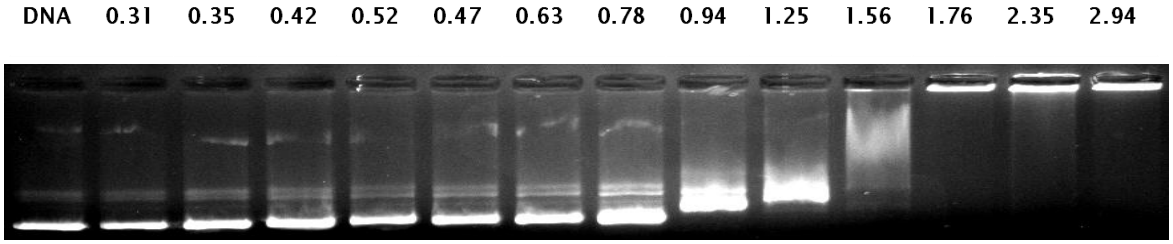

(b)

Figure 3.3: Gel Agarose Electrophoresis for: (a) E14 and (b) E10

The amount of polymer increases from left to right with DNA only in the far left well. The DNA and copolymer was mixed together in a vial and allowed to complex. The mixture was added to each well compared against the well which contained DNA only after running the agarose gel. The negatively charged DNA would migrate down the gel towards the positive electrode and the well with DNA only was used as a standard. As the amount of copolymer was added, the results show that the mixture would not migrate towards the positive electrode as far down as the DNA only well. Furthermore, as the copolymer was increased the polymer/DNA mixture did not migrate down the gel at all and stayed inside the well. These results suggest that as the amount of copolymer is increased the surface of the polyplex becomes more cationic. From these results it can be

inferred that the copolymer effectively condenses DNA which was consistent with prior results where polyplex formation with poly(MPC) block copolymers was studied. [17]

3.3.2 Gene delivery efficacy in liver hepatocellular carcinoma cells

The samples were mixed with DNA and the polyplexes were assessed for gene delivery efficacy in Hep G2 cells using (β-galactose). Each sample was tested to evaluate the effect of polymer/DNA (P/D) mass ratio on gene expression and was quantified by the production of ONP by measuring the absorbance at λ= 420nm. Branched Polyethyleneimine (PEI) is well-established for non-viral gene delivery systems and was used in this work as a positive control to compare with transfection efficiencies of the copolymers. Untreated cells and naked DNA was also used as additional controls. [18]

The gene expression of the copolymers was found to be relatively low irrespective of the molecular weights and compositions. Previous studies have shown that similar cationic phosphorylcholine polymers have shown some transfection in mammalian cells [15, 20]. Hyperbranched structures are usually larger in diameter than their linear counterparts because of the cascade-branched like structure and as a result could possibly form aggregates. This could explain the significantly lower gene expression of hyperbranched cationic phosphorylcholine polymers compared to block copolymers because of the limitations of particle size required for cellular uptake through endocytosis. Based on previous studies, it was found that by increasing the cationic component of the polyplex, the presence of charged groups could improve the electrostatic interactions between the polyplex and the cell membrane without compromising the fundamental biocompatibility of the copolymer. [19] A recent study evaluated the effect of calcium ions on the surface

potential of zwitterionics. [21] The surface potential of the zwitterionic lipids became positive as the Ca^{2+} concentration was increased. There was an immediate increase in surface potential from 0 to 0.1 mM Ca^{2+} concentration and then a gradual increase from 0.1 to 10 mM Ca^{2+}. The cationic surface potential can be explained by the Ca^{2+} interacting with the anionic phosphate group resulting in an increased cationic surface potential. It was hypothesized that dissolving the hyperbanced cationic phosphorylcholine polymers in calcium chloride would increase the cationic nature of the MPC component which would result in a more cationic surface potential for the copolymer. Various concentrations of calcium chloride were evaluated, however by dissolving the copolymers in a 15mM $CaCl_2$ solution instead of water before complexation with DNA, the samples showed a significant improvement in gene expression. Figure 3.4 shows gene expression as a function of copolymer dissolved in 15mM $CaCl_2$ solution to molecular weight. Copolymers of low molecular weights (M_n ~6 kDa) and (M_n ~ 15 kDa) showed significant gene expression and higher molecular weights (M_n ~33kDa) showed no gene expression which is a relatively similar result to the study done with poly(MPC) block copolymers. [16]. This significant improvement in transfection could be explained by the increased cationic surface potential of the copolymer which resulted in increased binding affinity of the copolymer to the nucleic acid which would make the polyplex more stable resulting in increasing transfection efficiency. Another possible explanation could be the increased electrostatic interactions between the polyplex and the cell membrane which could help facilitate cellular uptake resulting in increased transfection efficiency.

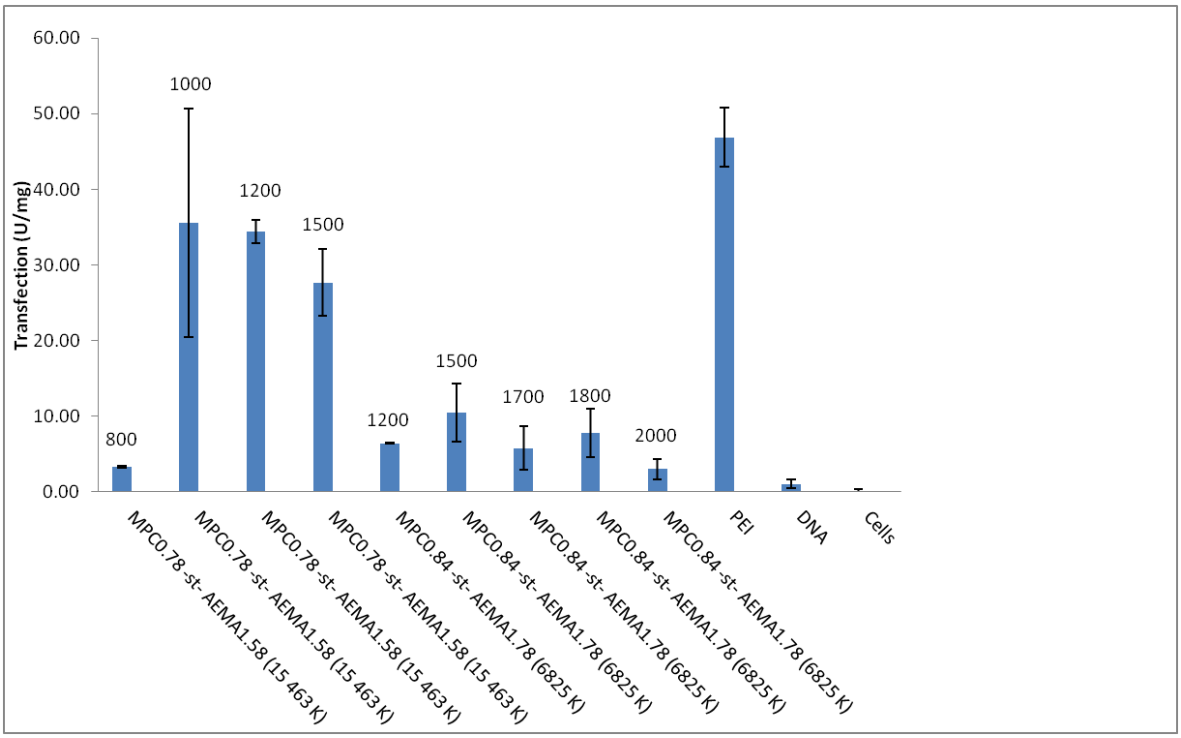

Figure 3.4: Gene expression of hyperbranched polymers in the presence of 15mM $CaCl_2$.

The polymer/DNA mass ratios are indicated by the number above the columns

References

[1] Boyer, C., Bulmus, V., Davis, T. P., Ladmiral, V., & Liu, J. (2009). Bioapplications of RAFT Polymerization. *Chemical Reviews*, 109(11), 5402-5436.

[2] Thurecht KJ, Blakey I, Peng H, Squires O, Hsu S, Alexander C, Whittaker, AK (2010). Functional Hyperbranched Polymers: Toward Targeted *in Vivo* ^{19}F Magnetic Resonance Imaging Using Designed Macromolecules.*J Am Chem Soc*,132(15), 5336–5337.

[3] Bhuchar, N., Deng, Z., Ishihara, K., & Narain, R. (2011). Detailed study of the reversible addition–fragmentation chain transfer polymerization and co-polymerization of 2-methacryloyloxyethyl phosphorylcholine. *Polymer Chemistry*, *2*(3), 632-639.

[4] Deng, Z., Li, S., Jiang, X., & Narain, R. (2009). Well-Defined Galactose-Containing Multi-Functional Copolymers and Glyconanoparticles for Biomolecular Recognition Processes. *Macromolecules*, *42*(17), 6393-6405.

[5] .Luzon M, Boyer C, Peinado C, Corrales T, Whittaker M, Tao L, Davis TP. (2010) Water-soluble, thermoresponsive, hyperbranched copolymers based on PEG-methacrylates: synthesis, characterization, and LCST behavior. *J Polym Sci, Part A: Polym Chem*, 48(13),2783–2792.

[6] Wang W-J, Wang D, Li B-G, Zhu S. (2010) .Synthesis and characterization of hyperbranched polyacrylamide using semibatch reversible addition-fragmentation chain transfer (RAFT) polymerization. *Macromolecules,*43(9), 4062–4069.

[7] Bhuchar, N., Sunasee, R., Ishihara, K., Thundat, T., & Narain, R. (2012). Degradable thermoresponsive nanogels for protein encapsulation and controlled release. *Bioconjugate chemistry*, *23*(1), 75-83

[8] Ahmed, M., Lai, B. F. L., Kizhakkedathu, J. N., & Narain, R. (2012). Hyperbranched Glycopolymers for Blood Biocompatibility.*Bioconjugate Chem*, 23(5), 1050-1058.

[9] Dong, Z.-min, Liu, X.-hui, & Li, Y.-sheng. (2009). Synthesis and Characterization of Hyperbranched Vinyl Polymers From Raft Polymerization of an Asymmetric Divinyl Monomer. *Chinese Journal of Polymer Science*, *27*(02)

[10] Malmström, E., & Hult, A. (2006). Journal of Macromolecular Science , Part C : Polymer Reviews Hyperbranched Polymers : *Glass*, (June 2012), 37-41.

[11] Ishihara, K., and Inoue, Y. (2010) Essential factors to make excellent biocompatibility of phospholipid polymer materials. *Advanced Science and Technology*. 76(1), 1–9.

[12] Ishihara, K., Goto, Y., Matsuno, R., Inoue, Y., and Konno, T.(2011) Novel polymer biomaterials and interfaces inspired from cell membrane functions. *Biochimica et Biophysica Acta* 1810(3), 268–275.

[13] Ishihara, K. (2000). Advanced Bioinspired phospholipid polymer biomaterials for making high performance artificial organs. *Science and Technology of Advanced Materials*, 1(3) 131-138.

[14] Lewis, A. L. (2000). Phosphorylcholine based polymers and their use in the prevention of biofouling. *Colloids Surface B: Biointerface*, 18(3-4) *131*.

[15] Ahmed, M., Bhuchar, N., Ishihara, K., & Narain, R. (2011). Well-controlled cationic water-soluble phospholipid polymer-DNA nanocomplexes for gene delivery. *Bioconjugate Chemistry*, *22*(6), 1228-38.

[16] Licciardi, M., Giammona, G., Du, J., Armes, P. S., Tang, Y., and Lewis, L. A. (2006). New folate-functionalized biocompatible block copolymer micelles as potential anti-cancer drug delivery systems. *Polymer* , 47(9), 2946–2955.

[17] Chim, Y. T. A., Lam, J. K. W., Ma, Y., Armes, S. P., Lewis, A. L., Roberts, C. J., Stolnik, S., et al. (2005). Structural Study of DNA Condensation Induced by Novel Phosphorylcholine-Based Copolymers for Gene Delivery and Relevance to DNA Protection. *Langmuir*, 21(8), 3591-3598.

[18] Boussif, O., Lezoualc'h, F., Zanta, M. a, Mergny, M. D., Scherman, D., Demeneix, B., & Behr, J. P. (1995). A versatile vector for gene and oligonucleotide transfer into cells in culture and in vivo: polyethylenimine. *Proceedings of the National Academy of Sciences of the United States of America*, *92*(16), 7297-7301.

[19] Palmer, R. R., Lewis, A. L., Kirkwood, L. C., Rose, S. F., Lloyd, A. W., Vick, T. a, & Stratford, P. W. (2004). Biological evaluation and drug delivery application of cationically modified phospholipid polymers. *Biomaterials*, *25*(19), 4785-4796.

[20] Sakaki, S., Tsuchida, M., Iwasaki, Y., and Ishiara, K. (2004) A water-soluble phospholipid polymer as a new biocompatible synthetic DNA carrier. *Bull. Chem. Soc. Jpn.* 77(12), 2283–2288.

[21] Perttu, E. K., Kohli, A. G., & Szoka, F. C. (2012). Inverse-phosphocholine lipids: a remix of a common phospholipid. *Journal of the American Chemical Society*, *134*(10), 4485-4488.

Conclusion and Future Work

The first part of this thesis presents the synthesis of cationic phosphorylcholine polymers via RAFT polymerization. The effect of different cross-linkers on molecular weight distribution was evaluated and it was found that *N*,*N*'-Methylene-bis-acrylamide resulted in broad molecular weight distributions greater than 1.5. The cationic phosphorylcholine polymers showed effective binding to DNA at varying polymer/DNA mass ratios and therefore have the potential to be used as gene delivery vectors. Current studies have attempted to transfect Hep G2 cells but the gene expression was found to be lower than polyethyleneimine (PEI) which was used as a standard. The gene expression was found to improve slightly in the presence of calcium chloride

Future studies are required to identify the possible barriers to high gene expression of those cationic phosphorylcholine polymers.

Part 2: Synthesis and Characterization of Conductive Elastomeric Polymer for Cardiovascular Applications

Introduction

The second part of this thesis is divided into three chapters:

Chapter 4 will discuss Poly(p-phenylene vinylene) (PPV): the basic structure and the synthesis protocols. PPV has a conjugated backbone structure which gives it unique electrical properties. The synthesis of the precursor monomer and polymerization were carried out as previously reported. The polymerization is followed by a thermal elimination reaction which gave the polymer the conjugated structure. This reaction is poorly understood and was studied by Shah and Arbuckle who proposed a mechanism and possible structure which is briefly discussed. The history, structure, electronic and mechanical properties of carbon nanotubes are explored as well as a general overview on Polydimethylsiloxane (PDMS).

Chapter 5 gives a brief overview of the instrumentation and experimental methods. Fourier Transform Infrared Spectroscopy (FTIR) and Thermogravimetric analysis (TGA) were used to characterize PPV and are briefly examined. The materials and methods to synthesize PPV/PDMS and MWNT/PDMS composite films are discussed as well as the procedures to synthesize them.

Chapter 6 will present the characterization results on PPV and the effect of cross linking agent and catalyst on the viscosity of PDMS film. The results of the composite films will be presented as well as the ongoing and future work.

4. Literature Review

4.1 Poly(p-phenylene-vinylene)

4.1.1 Overview of Conductive Polymers

Conductive polymers started in the 1960s with Paul Kurta but it wasn't until 1977 that their conductivity was reported by McDiarmid, Heeger and Shirakawa. [1] There conductivity is based around a conjugated backbone structure and their applications range from: buttons, organic light emitting diodes, sensors, molecular wires and actuators. [2-8] Electrical conductivity usually ranges between 10^{-10}-10^{-5} S cm^{-1}, however they can be doped to produce conductivities in the range of 1- 10^{-5} S cm^{-1}. [1] Interest is now growing towards understanding their physical and chemical properties in a doped or undoped state. [3]They are organized into three different categories: metals, semiconductors and insulators. Conductive polymers are generally classified as semiconductors but in some cases they can be highly conductive such as in the case of polyacetylene. [3] There are two different methods to synthesize conductive polymers: chemical and electrochemical polymerization. [9]

PPV is a conductive polymer which is conductive by the addition of electron donors or acceptors due to its conjugated structure. [1] There are several synthesis methods but the most common is the base induced polymerization of a sulfonium salt monomer in aqueous solution and will be elaborated in the latter sections. The final structure of a PPV repeat unit is shown below in Figure 4.1.

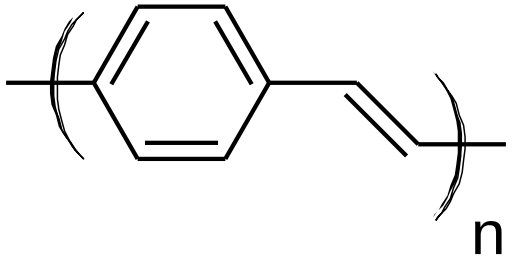

Figure 4.1: Structure of Poly(p-phenylene-vinylene)

4.1.2 Synthesis of Poly(p-phenylene-vinylene)

Burn and Bradley synthesized PPV with several precursor routes. Different precursor polymers give different structural and electronic properties but this review will cover the scheme shown in Figure 4.2.

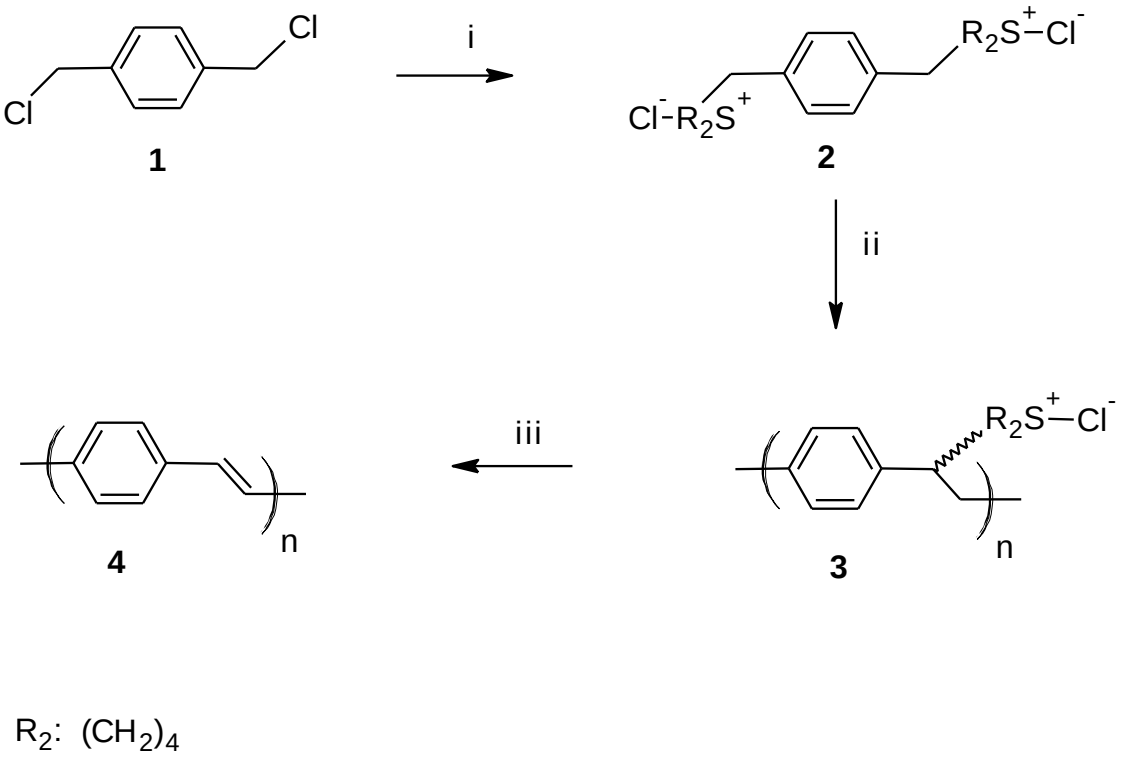

Figure 4.2: Synthetic Pathway to PPV

The monomer p-phenylenedimethyl-ene- 1,1-bis(tetrahydrothiophen-1-ium) dichloride **2** was synthesized by reacting **1** with tetrahydrothiophene (THT) in a argon or nitrogen environment. The polymerization is carried out using methanol as a solvent and is done in an argon or nitrogen environment to prevent unwanted side reactions. Sodium hydroxide was slowly added to the monomer **2** to obtain Poly (p-phenylene [1 - (tetrahydrothiophen-1-io) ethylene chloride)] **3.** The polymerization is terminated by neutralization with the slow addition of HCl and the product is dialyzed against water to remove all salts. **3** is then converted into the conjugated polymer PPV **4** via a thermal elimination reaction by heating the film under a vacuum at 220- 250°C for 12 hours. [9]

The thermal elimination reaction has been studied in cyclic sulfides and is a poorly understood because it involves several mechanisms but was studied by Shah and McGhie. They coupled mass spectrometry (MS) and thermal gravimetric analysis (TGA) to keep experimental variables such as sample size and shape, ambient atmosphere, flow rate, temperature, heat and mass transfer effects essentially the same for each experiment

allowing for the direct comparisons of results. [11]

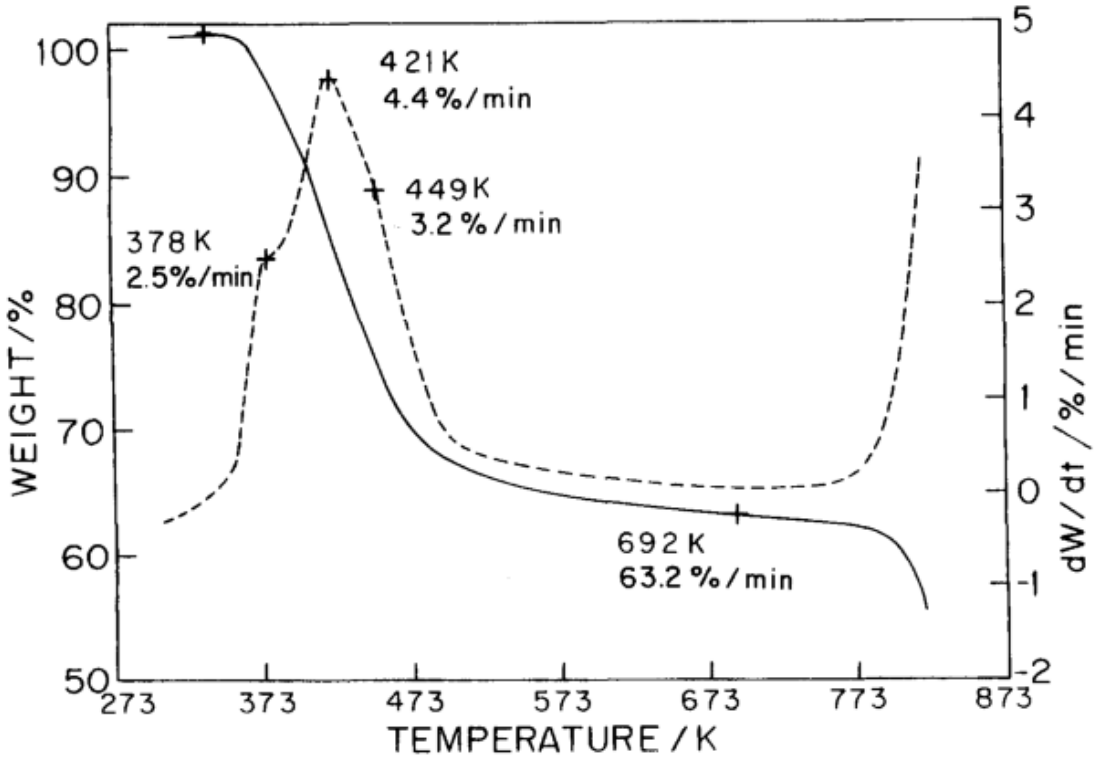

Figure 4.3a: TGA data of a of evolved products of thermal elimination reaction [11]

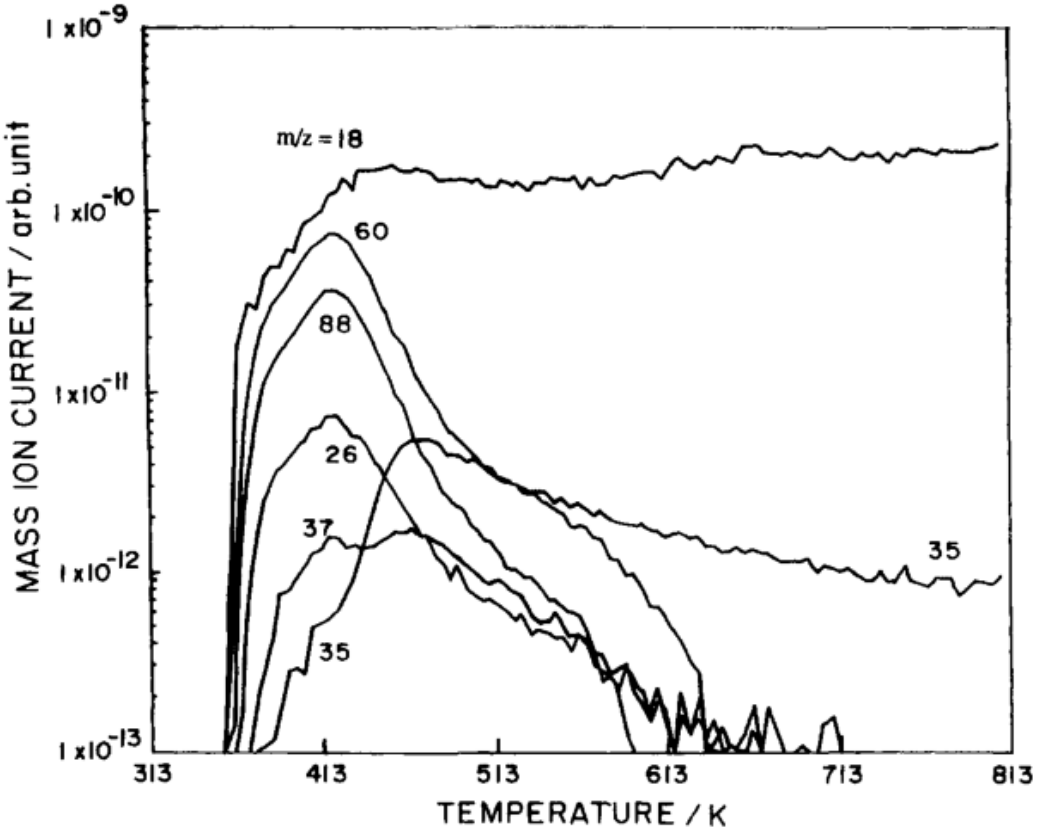

Figure 4.3b: MS of evolved products of thermal elimination reaction [11]

The MS shows that the first product to leave is water, then the THT including its fragments C_2H_4S and C_2H_2. The corresponding TGA plot shows weight loss starting at 373K with the loss of water first and then THT is eliminated at 378K which is shown by the shoulder on the DTG plot. These results show evidence that the thermal elimination reaction is not a single step but rather a two step process. The MS shows that the first product to be eliminated is THT which is consistent with the E1 mechanism. [11] It was proposed by Massardier [12] that a C-Cl intermediate species is formed, but is not possible because according to Figure 4.3b the elimination of chlorine happens at a

temperature that is too low to break the C-Cl covalent which would require a temperature of 533K- 573K. It was proposed by Shah that due to the presence of water it provides a pathway for a competing substitution (S_N1) reaction which results in the formation of a hydroxyl substituent in the final product [4]. The proposed reaction mechanism is shown in Figure 4.4.

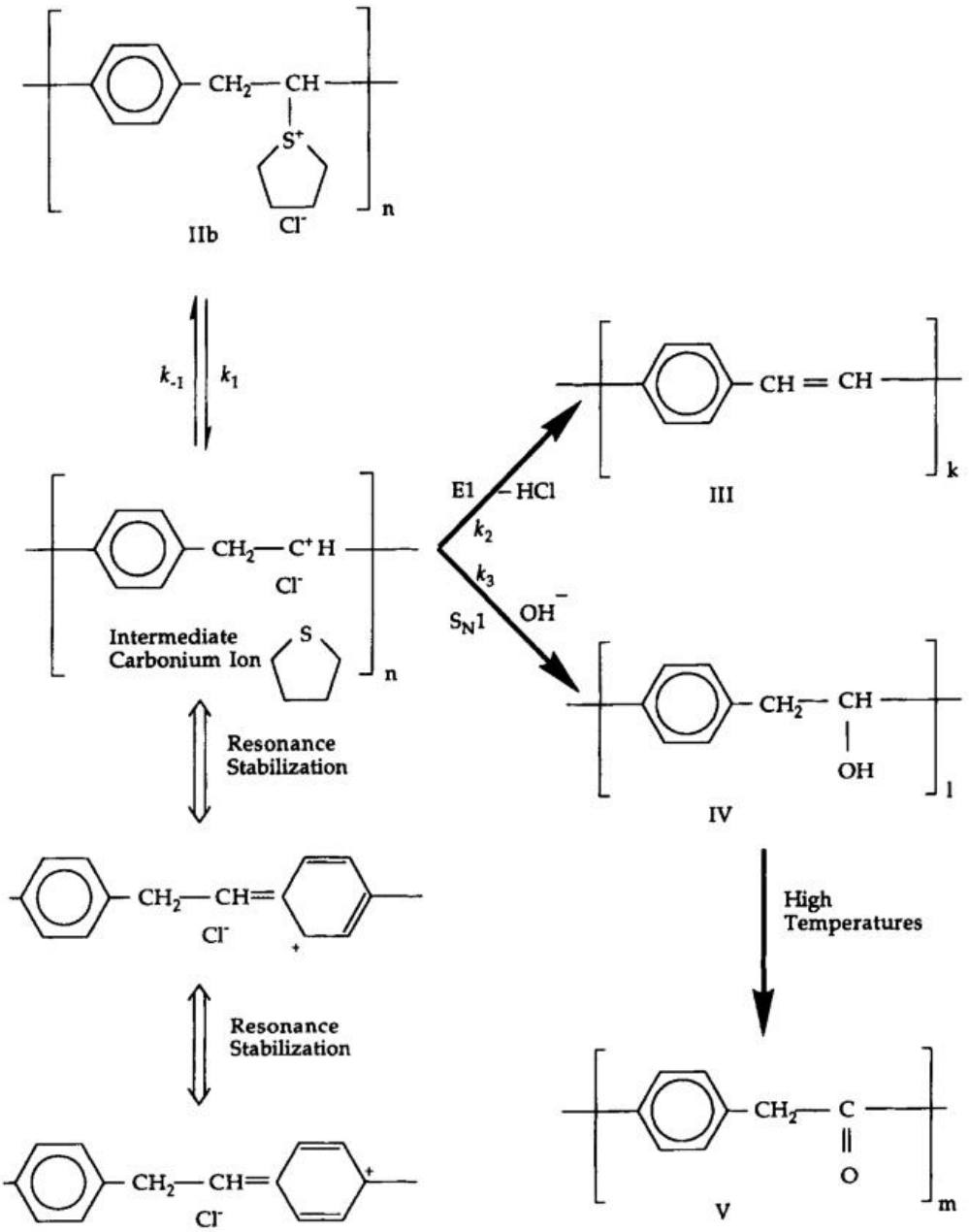

Figure 4.4: Proposed PPV thermal elimination reaction mechanism [11]

The final proposed structure of PPV is given in Figure 4.5:

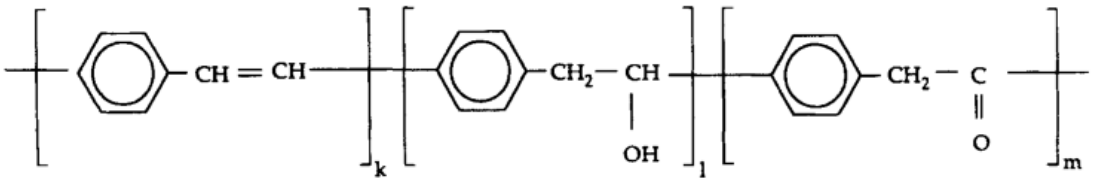

Figure 4.5: Final proposed PPV structure with impurities [11]

4.2 Carbon Nanotubes

4.2.1 History

Carbon nanotubes are a form of fullerenes which are large, closed cage, carbon clusters. Fullerenes were accidently discovered in 1985 by Kroto and Smalley [13] when they found strange results in the mass spectra of evaporated carbon samples, but were first reported in 1991 by Iijima [14] and coworkers and have since been investigated by many researchers all over the world. [15]

4.2.2 Structure of Carbon Nanotubes

There are two different types of carbon nanotubes: single walled nanotubes (SWNT) and multi walled nanotubes (MWNT). SWNT are wrapped graphene sheets while MWNT are a collection of concentric tubes of graphene. [15] Graphene is a flat layer of carbon atoms packed into a two dimensional honeycomb lattice which can be arranged in pentagons and hexagons which can then also be ordered in either: armchair, zigzag or chiral orientations. [15, 16] The three different orientations are shown in Figure 4.6.

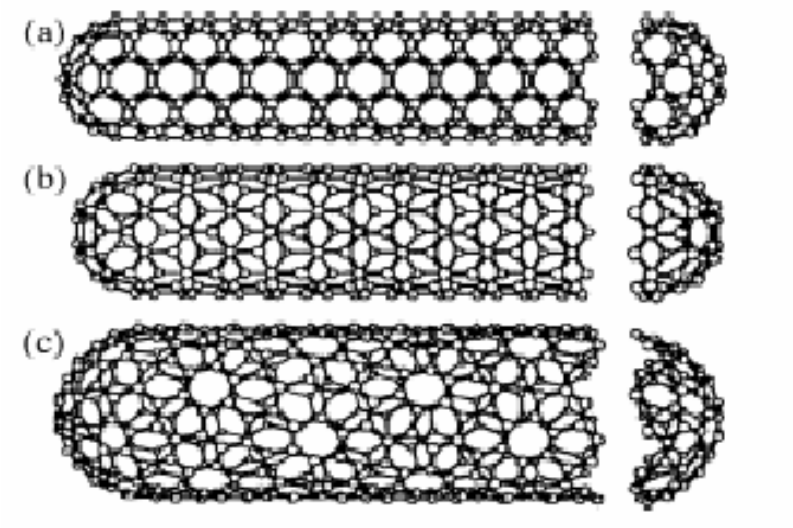

Figure 4.6: Different nanotubes structures: (a) armchair (b) zigzag (c) chiral [15]

The different structures shown in Figure 4.6 depend on how the graphene sheet is rolled up. When a sheet is rolled up to form a closed cylinder, two atoms in the sheet are chosen, one which serves as the origin. The sheet is rolled until the two atoms coincide and the vector that points from the origin to the other atom is known as the chiral vector and its length is equal to the circumference of the cylinder. The chiral vector determines how the sheet is rolled which consequently affects the structure and properties of the carbon nanotube. [15] The geometry of the sheet is shown in Figure 4.7. Geometries of carbon nanotubes are mapped out using a (n,m) grid where n represents the horizontal position and m the vertical position. For the zig-zag structure, m=0 and as a result the chiral vector is a horizontal line. Similarly, when n=m the structure ends up being armchair and any other values of n and m result in a chiral structure. [17]

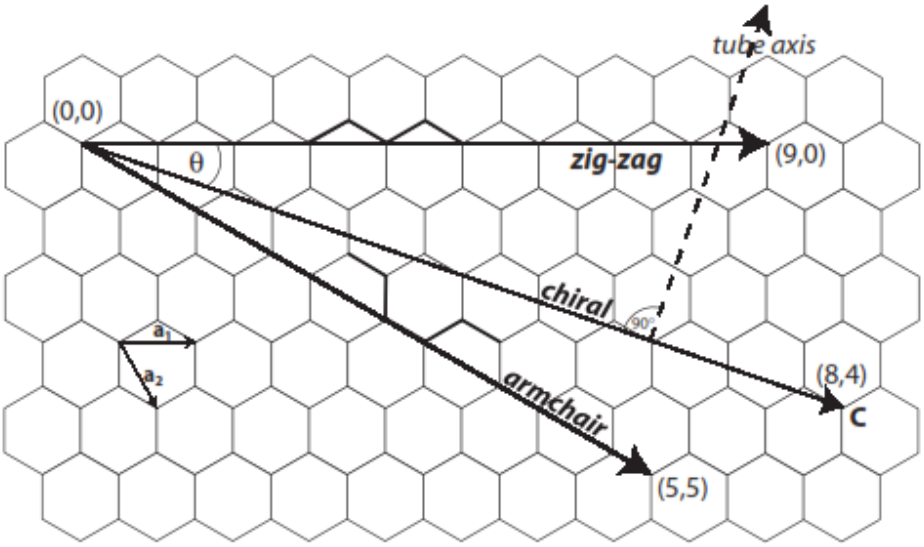

Figure 4.7: Carbon nanotube geometry [16]

4.2.3 Electronic Properties

Electrical properties of carbon nanotubes can be explained by the band folding scheme. Conductance is only possible when the π and π^* orbital's overlap, which is the case in high symmetry. [17] Figure 4.8 is an energy dispersion diagram of hexagonal carbon atoms and includes the points of high symmetry (K). When the chiral vector crosses the K point system will show conductance, when he K point is not included it is a semiconductor. [18]

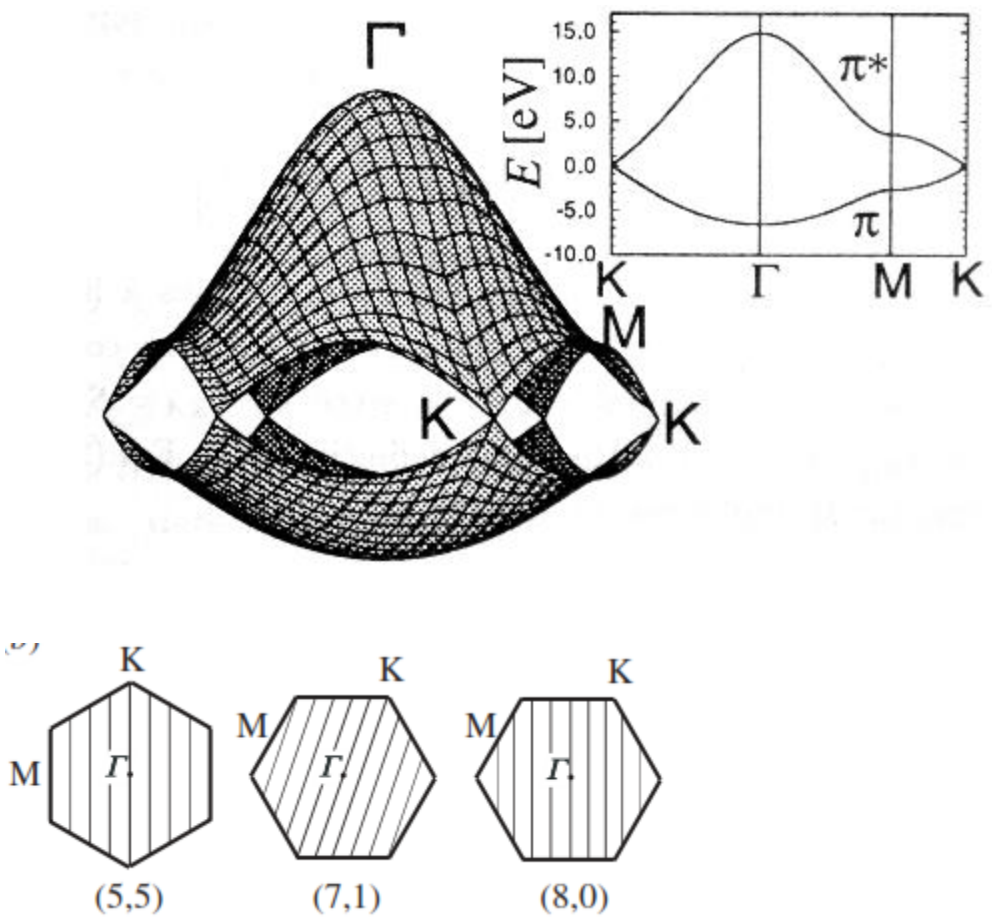

Figure 4.8: Energy dispersion diagram [8]

The closer the chiral vector is to crossing through the points of high symmetry the closer the system gets to having metallic conductance. [17] This is shown in Equation 1:

$$n - m = 3j \tag{1}$$

For integer values of j, the system would be considered metallic because of curvature effects, which lead to energy gaps that affect conductance. There are three different types of energy gaps: zero gaps, tiny gaps and large gaps which all correspond to different values of j. Zero gaps are when j is zero and are in the cases of armchair structures, when

j is a non-zero integer it means there are tiny energy gaps and they usually indicate semiconducting behavior. All other values of j are large gaps and are almost always associated with semiconducting behavior. [19]

4.2.4 Mechanical Properties

Carbon nanotubes have special mechanical properties that make them ideal reinforcing agents due to their high modulus and low weight of the fibers. Krishnan and Dujardin reported a Young's modulus of 1 TPa which was higher than steel at 200 GPa. Similar values were given for tensile strength of 10-150 GPa which beats steel with 0.4 GPa by far. The values were higher for MWNT than for SWNT. [19]

The final mechanical properties of a composite material depend on the load transfer and adhesion between the matrix and the filler. [20] Wager [21] dispersed MWNT into different polymers and found through a tensile test that the fractures were at the holes in the polymer matrix rather than at the gripping regions at the end of the bundles. This suggested that the MWNT provided significant load transfer and interfacial adhesion when used as a reinforcing agent in polymers.

4.3 Polydimethylsiloxane

4.3.1 General Overview

Polydimethylsiloxane (PDMS) is a type of elastomer that has excellent biocompatibility and is typically used as a food additive in antifoaming or anti caking agents. PDMS consists of a linear siloxane backbone and is shown below in Figure 4.9. [22]

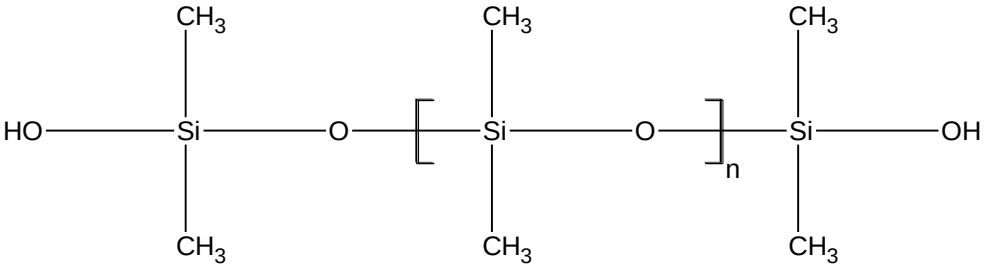

Figure 4.9: Structure of Polydimethylsiloxane

The biocompatibility of PDMS is a because of the molecular structure of dimethylsiloxane. The Si-O bond is stable because of a high bond energy and as a result the polymer is stable in biological media. Chemical and thermal stability not only make the polymer non-biodegradable but sterilized by steam. An open molecular structure results in the polymer being permeable to molecules such as oxygen and stream. . Additional properties such as anti adhesive and water repellent properties decrease the molecular and cellular adhesion as well as the elasticity which reduces tissue stress. [23]

PDMS has a low glass transition temperature, a shear modulus of G= 250 kPa and is non toxic to humans. [22] It is the most flexible polymer making it attractive for cyclic loading applications. There have been some studies to date which have looked at

embedding conductive polymers or reinforcing agents into PDMS to improve the electrical and mechanical properties.

4.3.2 Electromechanical effect of PPV/PDMS composites

Niamlang and Srivat studied the electromechanical properties of a PPV/PDMS composite film to be used for actuator applications. PPV was synthesized by the methods mentioned in Burn and Bradley and characterized using Fourier Transform Infrared Spectroscopy (FTIR) and Thermal Gravimetric Analysis (TGA). 5, 7, 10, 15 and 20 wt % fractions of PPV were embedded into PDMS and there electromechanical properties were tested. [24]

The PPV showed peaks at 3022, 550, 830 and 1511 cm^{-1} and the TGA showed one degradation step at 554°C. [25]

The effect of an electric field on the storage modulus (G') was studied at an electric field strength (E) of 1 kV mm^{-1} and 2 kV mm^{-1}. Figure 4.10 shows the storage modulus

response of PPV/PDMS-10 when the electric field was switched on and off. [24]

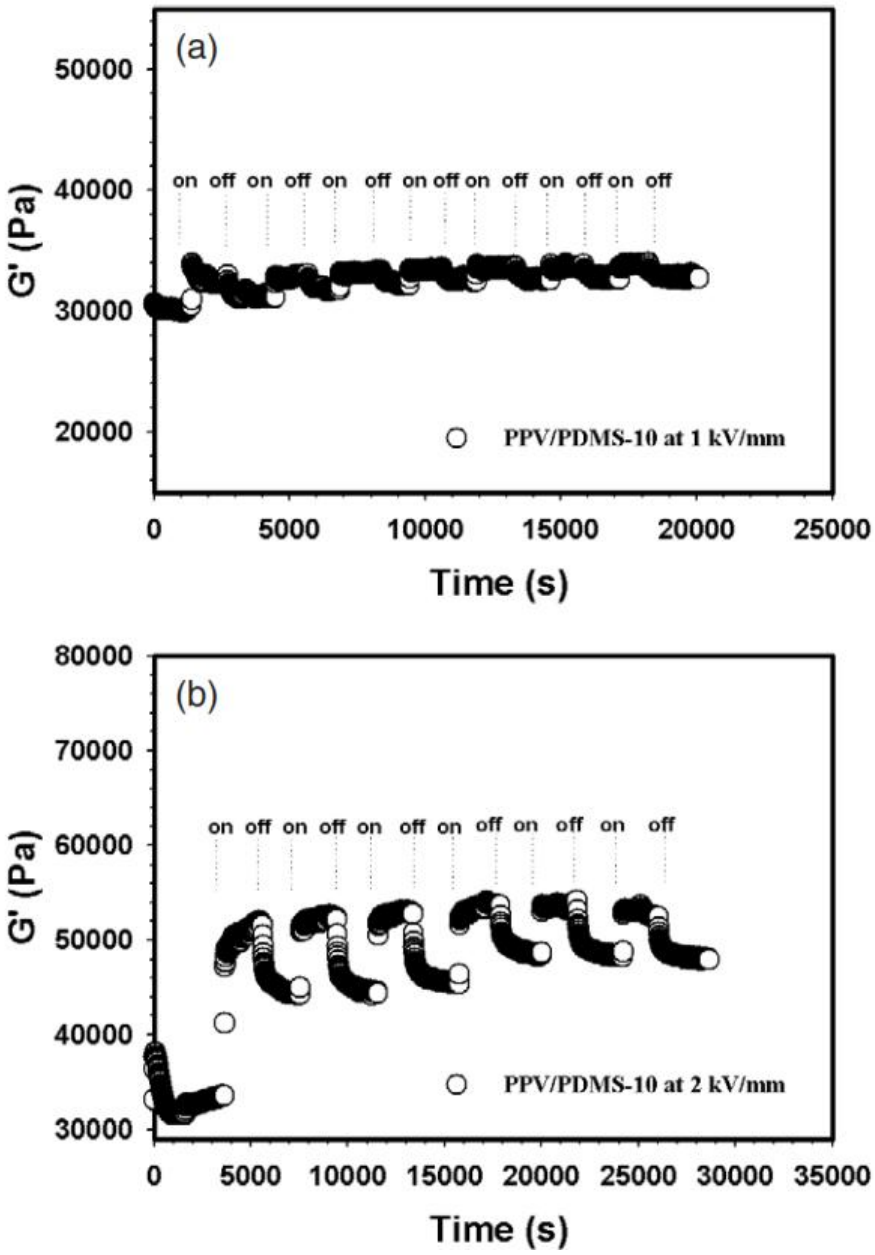

Figure 4.10: Storage modulus response of PPV/PDMS-10 to an electric field strength of (a) 1 kV mm^{-1} (b) 2 kV mm^{-1} [24]

At 1 kV mm^{-1} when the electric field was turned on the G' reached a steady state, but when it was turned off the system recovered its original G' value. This was explained by the induced dipole-dipole interactions which are present when the electric field was turned on however would vanish when the field was turned off. The same was not true when the electric field was increased to 2 kV mm^{-1}. The PPV/PDMS appeared to show an increase in G' when the electric field was turned on but does not recover its original value when the field was turned off. This indicates that some of the induced dipole-dipole interactions remain as "residues within the PPV particles" which cause irreversible interactions. [24]

The time required for G' to reach a steady state was referred to as the induction time τ_{ind} and then τ_{rec} to recover back to its original value. The τ_{ind} and τ_{rec} was 278 seconds and 131 seconds for 1 kV mm^{-1} and were 78 seconds and 163 seconds for 2 kV mm^{-1} respectively. At high electric field strengths, the recovery time was larger because the PPV would trigger higher induced dipole moments which lead to higher residue dipole moments. The residues slowly decrease in strength and therefore a longer recovery time was required. [24]

4.3.3 Mechanics of MWNT/PDMS

Carbon nanotubes have excellent properties and are used as reinforcing agents in composite materials. Paul and Valiyaveetitil used a dynamic mechanical analyzer to study the mechanical properties of a MWNT/PDMS composite film. [25]

Figure 4.11 shows more stress is required to obtain the same strain when the weight fraction of carbon nanotubes is increased. As the weight percent of carbon nanotubes are

increased it results in a stiffer composite. The storage modulus increases by a factor of 1.3 at zero static stress and the difference in storage modulus at high stresses is 2.6 times larger in 10 wt % carbon nanotube. [25]

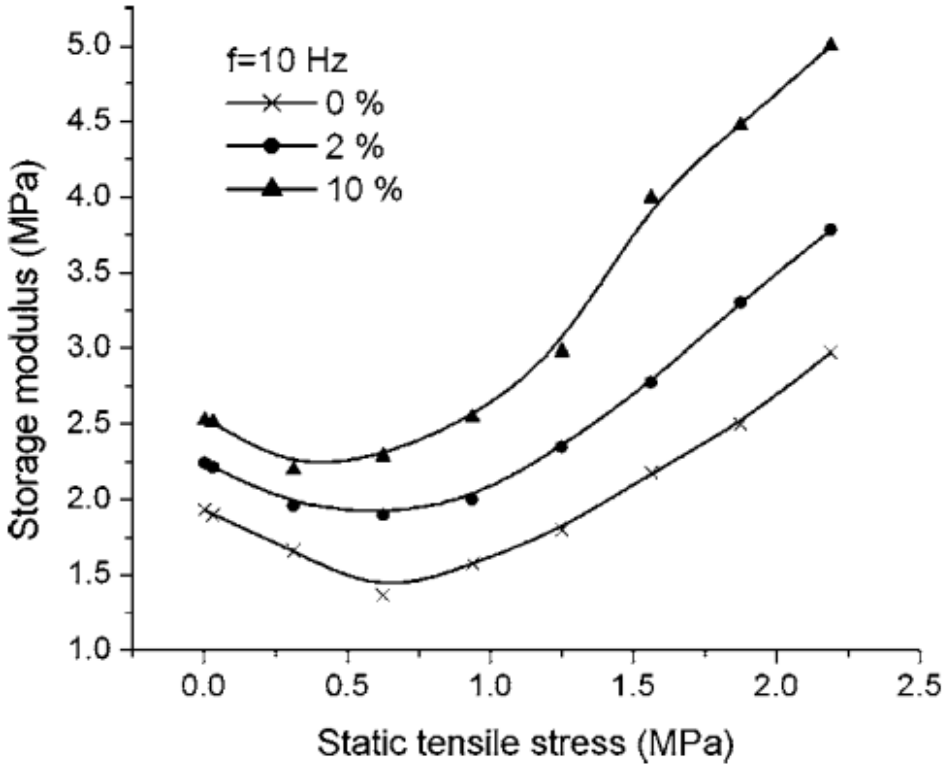

Figure 4.11: Effect of tensile stress on the storage modulus of MWNT/PDMS composite for different weight fractions of nanotubes [25]

References

[1]Ballantyne, A. M. (2005). *Functionalised Polythiophenes: Synthesis, Characterisation and Application*. Massey University.

[2] Kraft, A., Grimsdale, A. C., & Holmes, A. B. (1998.). Electroluminescent Conjugated Polymers Seeing Polymers in a New Light. *Angew. Chem. Int. Ed, 37(4),402-428.*

[3] Roncali, J.. (1992).Conjugated Poiy(th1ophenes): Synthesis, Functionalizatlon, and Applications. *Chem Rev.* 92(4), 711-738.

[4] Beauprø, B. S., & Leclerc, M. (2002). Fluorene-Based Copolymers for Red-Light-Emitting Diodes, 12 (3), 192-196.

[5] Poly, A.-functionalized, Reddinger, J. L., & Reynolds, J. R. (1997). Ultraviolet-Emitting, Alkoxy-Functionalized Poly(m-phenylene). *Society*, *9297*(96), 479-481.

[6] Grant, D. K. (2003). *The synthesis and properties of polyether substituted oligothiophene*. Massey University.

[7] Jones, W. E., Jr. ; Dong, H.; Nyame, V.; Ochanda, F. (2003). Conducting molecular nanofibres and nanotubes for electronics applications. *61st Annual Technical Conference* (pp. 1948-1950). Nashville, TN.

[8] Anquetil, P. A; Hunter, I.; Madden, J. D.; Madden, P. G. ; Pullen, A; Swager, T. M.; Xu, B.; Vu, H.-H. . (2003).

[9] Burn, P. L., Bradley, D. D. C., Friend, R. H., Halliday, D. a., Holmes, A. B., Jackson, R. W., & Kraft, A. (1992). Precursor route chemistry and electronic properties of poly(p-phenylenevinylene), poly[(2,5-dimethyl-p-phenylene)vinylene] and poly[(2,5-dimethoxy-p-phenylene)vinylene]. *Journal of the Chemical Society, Perkin Transactions 1*, 1992(23), 3225-3231.

[10] Uc, Z. K., & East, M. (2003). Synthesis, Characterization and Electrical Conductivity of Poly (p-phenylene vinylene). *Turkish Journal of Chemistry*, *27(2)*, 135 - 143.

[11] Shah, H.,& Arbuckle, G. (1996). A study of the thermal elimination reaction in a poly(p-phenylene vinylene) prescursor. *Thermochimica Acta*, *287(2)*, 319-326.

[12] Massardier, V., Hoang, T. V., & Guyot, A. (1994). Thermal Elimination Reaction in Polyparap henylene Vin ylene Synthesis from the Soluble Sulfonium Salt Precursor Route. *Polymers for Advanced Technologies*, *5(10)*, 656-663.

[13] H.W.Kroto, J.R.Heath, S.C.O'Brien, R.F.Curl, and R.E Smalley, (1985). C_{60}: Buckminsterfullerene. *Nature*, 318(6042), 162-163.

[14] Iijima, Sumio, (1991). Helical microtubules of graphitic carbon. *Nature*, 354(6348), 56-58.

[15] Daenen, M, de Fouw, R.D, Hamers, B, Janssen, P.G.A, Schoutedem, K. (2003). *The Wondrous World of Carbon Nanotubes* (p. 96).

[16] Geim, a K., & Novoselov, K. S. (2007). The rise of graphene. *Nature materials*, *6*(3), 183-91.

[17] Burtscher, L. (2005). *Electrical and mechanical properties of carbon nanotubes*. Heriot-Watt University.

[18] Venema, L. C., Wildo, J. W. G., & Dekker, C. (1998). Electronic structure of atomically resolved carbon nanotubes *Nature*, *584*(10), 1996-1999.

[19] Dresselhaus, B. M. S., Dresselhaus, G., & Charlier, J. C. (2004). Electronic , thermal and mechanical properties of carbon nanotubes. *Electrical Engineering*, 362(1823), 2065-2098

[20] Salvetat, J. P, Bonard, N.H, Thomson, N. H., Kulik, A. J., Benoit, W., & Zuppiroli, L. (1999). Mechanical properties of carbon nanotubes. *Applied Physics A Materials Science & Processing*, *260(3)*, 255-260.

[21] Wagner, H. D., Lourie, O., Feldman, Y., & Tenne, R. (1998). Stress-induced fragmentation of multiwall carbon nanotubes in a polymer matrix. *Applied Physics Letters*, *72*(2), 188-191

[22] FNP 34 (1986). Metals and arsenic specifications.

[23] Briquet, F., Colas, A., & Thomas, X. (1996). Silicones for medical use,

[24] Niamlang, S., & Sirivat, A. (2008). Dielectrophoresis force and deflection of electroactive poly(p -phenylene vinylene)/polydimethylsiloxane blends. *Smart Materials and Structures*, *17*(3), 1-9

[25] Paul, J., Sindhu, S., Nurmawati, M. H., & Valiyaveettil, S. (2006). Mechanics of prestressed polydimethylsiloxane-carbon nanotube composite. *Applied Physics Letters*, *89*(18),1-3

5. Instrumentation/Experimental Methods

5.1 Fourier Transform Infrared Spectroscopy (FTIR)

5.1.1 Theory

When infrared radiation is passed through a molecule it will begin vibrating to the next energy state only if it absorbs enough energy. However, infrared radiation will only absorb into the molecule at the same frequency the bond vibrates and will only absorb if the molecule can exhibit a change in the dipole moment. [1]

The two fundamental modes of vibration for molecules are stretching and bending. Stretching requires more energy and is present at high frequencies whereas bending requires less energy. If the vibration of the bond is compared to the oscillation of a spring, the phenomenon can be explained by Hooke's law which is shown in equation 2. If the strength of the bond is represented by k (spring constant) then the ω (frequency) will change with respect to the strength of the bond.

$$\omega = \frac{1}{2\pi}\sqrt{\frac{k}{\mu}} \tag{2}$$

When radiation is passed through the sample, some of it is absorbed and transmitted. The spectrum represents the molecular absorption and transmission which creates a molecular "fingerprint" that is unique to every compound.

5.1.2 Sample Analysis

Figure 5.1 shows the sample analysis process of the spectrometer and is explained below: [2]

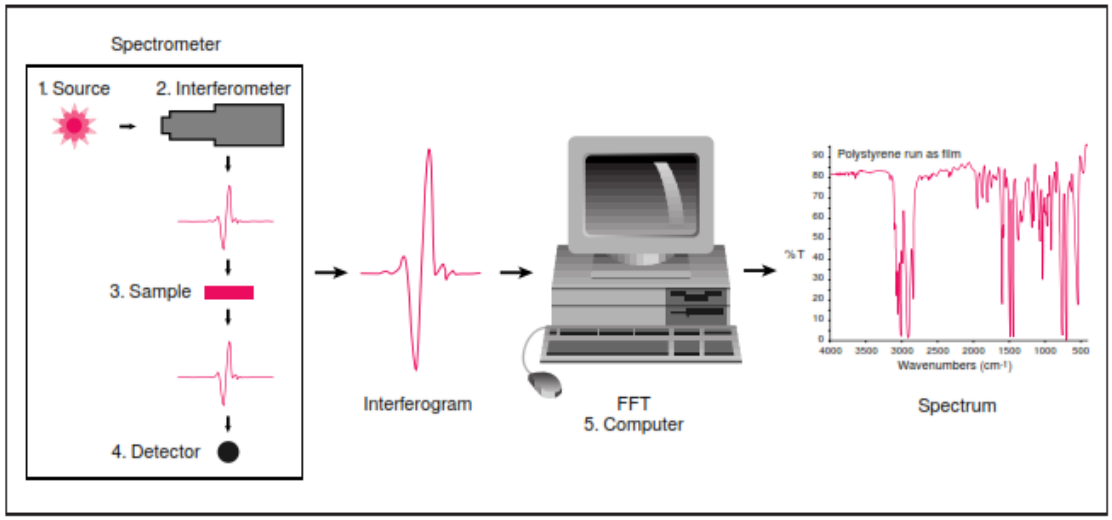

Figure 5.1: Sample analysis process [2]

1. Source: Infrared radiation is emitted from a source.

2. Interferometer: The beam enters the interferometer where spectral encoding takes place. The resulting interferogram signal exits the interferometer.

3. Sample: The beam enters the sample and is either transmitted or absorbed depending on what is being measured.

4. Detector: The beam passes to the detector which is designed to measure the signal from the interferogram.

5. Computer: The measured signal is sent to a computer where the Fourier transformation takes place.

Figure 5.2 shows a schematic diagram of the beam splitting which is unique to FTIR.

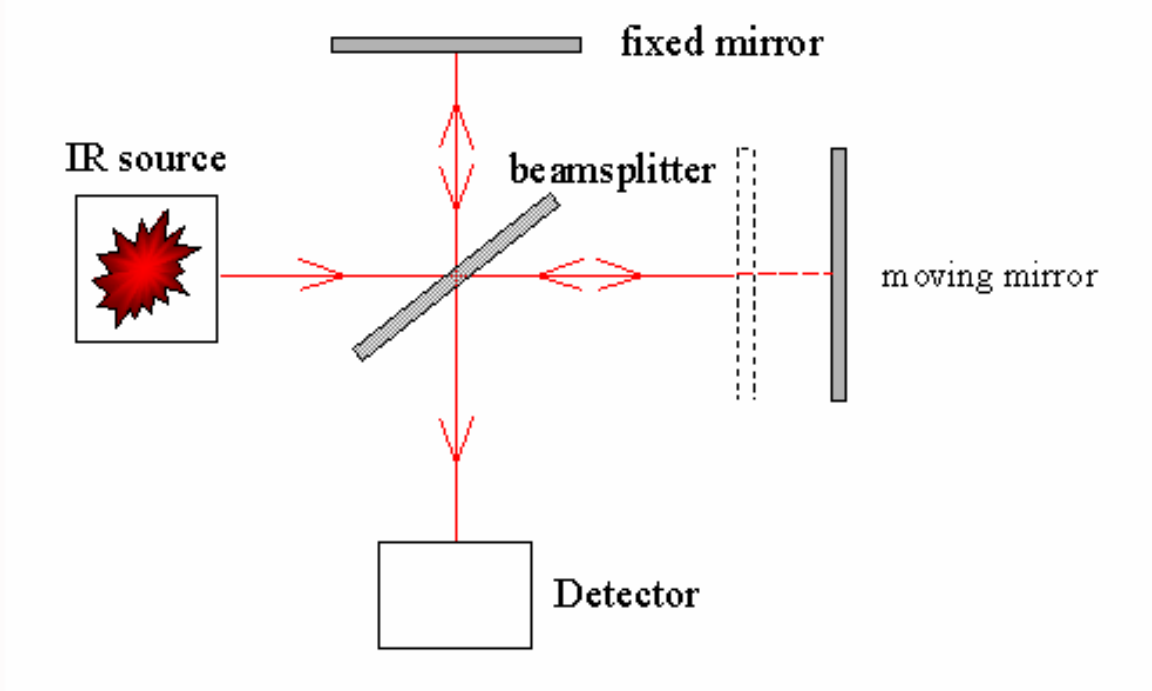

Figure 5.2: Schematic layout of moving mirror, beam splitter and detector [2]

Infrared light is passed through a beam splitter which splits 50% of the light to a stationary mirror and 50 % of the light to a moving mirror. The light is then reflected back from both mirror and combined. Depending on the position of the mirror, there are three configurations [1]:

- Zero Path Difference: If the moving mirror is the same distance from the beam splitter as the fixed mirror then 50% of the light would bounce off of each mirror and combine and the halves would be in exact phase with one another. This would give constructive interference and the detector would see a maxima.
- Destructive Interference: if the moving mirror is ¼ a wavelength greater than the distance of the fixed mirror, then when the two beams combine there would be destructive interference and the detector would see a minima.

- Constructive Interference: if the moving mirror is ½ a wavelength greater than the distance of fixed mirror, then the two beams would be in phase and there would be constructive interference and the detector would see a maxima.

The detector can see all the frequencies at once and so it sums up all the constructive and destructive interferences produced by the moving mirror and constructs an interferogram. The interferogram measures every data point as a function of the moving mirror and must be converted using Fourier transformation. [2]

FTIR has many advantages over infrared spectroscopy: it is non-destructive, provides precise measurement with no external calibration, increases speed and its mechanically simple with only one moving part. [2]

5.2 Thermogravimetric Analysis

Thermogravimetric analysis (TGA) is a technique where the weight loss is measured as a function of the temperature in a controlled atmosphere. TGA consists of two sample pans inside a furnace with a precision balance. One of the pans is used a reference weight and the other pan is to load the sample. Typically 2- 50mg of sample should be loaded to obtain an accurate measurement, however if there is a minimum amount of sample then 1 mg is enough. The mass of the sample is monitored while the furnace is heated or cooled by a sample purge gas. TGA can be used to quantify a variety of measurements such as: loss of water, loss of solvent, loss of plasticizer, decarboxylation, pyrolysis, oxidation, decomposition, weight % filler and amount of catalytic residue. [3]

5.3 Materials

α-α'-Dichoro-p-xylene, tetrahydrothiophene (THT), dibutyltin dilaurate and Tetraethyl orthosilicated (TEOS) and hydroxyl terminated polydimethylsiloxane were purchased from Sigma Aldrich. Multi-walled carbon nanotubes were purchased from Sun Innovations Inc. Acetone and methanol were used as received.

5.4 Methods

The FTIR spectrum was run on a Nicolet 8700 (Thermo) and potassium bromide was used to record the background signal. Thermal degradation was measured using a SDTQ 600 (TA instruments) with a heating rate of 10°C min^{-1} in a N_2 atmosphere. The thermal elimination reaction was carried out at the University of Alberta NanoFab Facility. PDMS curing was done using a vacuum oven

5.4.1 Synthesis of PPV

PPV was synthesized according to the method in Burn and Bradley. In a typical procedure 12 mL of THT was added to 4 g of α'-α dichloro-p-xylene in 100 mL of methanol. The mixture was degassed using nitrogen air and then heated in a 50°C oil bath overnight. 1.5 L of acetone was then poured over the mixture to precipitate p- p-phenylenedimethyl-ene- 1,1-bis(tetrahydrothiophen-1-ium) dichloride. Before filtration, the mixture was stirred in an ice bath for ½ hr before filtration. The monomer was collected through vacuum filtration at room temperature.

5.1 g of the washed and dried monomer phenylenedimethyl-ene- 1,1-bis(tetrahydrothiophen-1-ium) dichloride was dissolved in 43 mL of methanol and cooled

down to 0°C. 36 mL of sodium hydroxide was added drop wise for 20 minutes while the temperature was maintained at 0°C. The reaction was allowed to stir for an additional hour at 0°C and then was neutralized with 0.4M hydrochloric acid. The solution was then dialyzed against a 1L water-ethanol (1:1) mixture for three days using 13 000 MW cut-off dialysis tubing. The residue Poly (p-phenylene [1 - (tetrahydrothiophen-1-io) ethylene chloride)] was poured onto a glass dish and allowed to evaporate at room temperature in a free air stream for 24 hours. The yellowish green film was then placed in a vacuum oven at 220°C for 12 hours to obtain PPV.

5.4.2 Synthesis of PPV/PDMS

In a typical procedure 3.0 g of PDMS, 3.98 mg of PPV, 321.5 µL of TEOS and 28.5 µL of dibutyltin dilaurate was mixed into a 2.2 mL vial and stirred. The mixture was then poured onto a mold and placed a vacuum oven and allowed to cure under a pressure of 0.6 atm at 27°C for 4 hours. The polymer was left overnight to dry at room temperature and then peeled off the mold the next day.

5.4.3 Synthesis of CNT/PDMS

A stock solution of MWNT were prepared by mixing 1 g of MWNT in 10 mL of DMF and sonicated for 6 hours before they were mixed with PDMS. In a typical procedure 3.0 g of PDMS, 750 mg of MWNT, 321.5 µL of TEOS and 28.41 µL of dibutyltin dilaurate was mixed into a 2.2 mL vial and stirred. The mixture was poured onto a mold and placed into a vacuum oven and allowed to cure under a pressure of 0.6 atm at 27°C for 4 hours. The polymer was left overnight to dry at room temperature and then peeled off the mold the next day.

References

[1] Tissue, B. M.. FTIR Theory. *Thermo Electron Corporate Scientific Instruments Training Institute*.

[2] Nicolet, T., & All, C. (2001). Introduction to Fourier Transform Infrared Spectrometry.

[3] Thermogravimetric, T., & Family, I. (1960). Thermogravimetric Analysis (TGA) A Beginner ’ s Guide. *Analysis*.

6. Results and Discussion

Silicones are used in various medical applications due to their biocompatibility. The most commonly used silicones are PDMS and they are found in applications that involve contact with the human body. [1, 2] PPV was synthesized and characterized and was embedded into a PDMS matrix as well as MWNT.

6.1 Characterization of Poly(p-phenylene vinylene)

FTIR spectroscopy was done using KBr to obtain a baseline and the data is shown in Table 6.1.

Table 6.1: FTIR spectra data for PPV [3]

Functional Group	Wavelength (cm^{-1})	Reference
Trans vinylene group	3023	[1]
CH_3 asymmetric stretching	2945	[1]
CH_3 symmetric stretching	2734	[1]
C-C ring stretching	1517	[1]
C-H out of plane bending	963	[1]
Para phenylene ring C-H	863	[1]
Phenelyne out of plane ring bending	558	[1]

The bands at 3023 cm^{-1} can be attributed to the *trans* vinylene C-H stretching. 2734 cm^{-1} and 2945 cm^{-1} are assigned to CH_3 symmetric and asymmetric stretching respectively. The bands at 1517 cm^{-1} are due to C-C ring stretching. 963 cm^{-1} is assigned to C-H out of

plane bending which indicates a *trans* configuration of the vinylene group. 863 cm^{-1} and 558 cm^{-1} correspond to para-phenylene ring C-H out of plane bending and phenylene out of plane ring bending respectively. [3] The thiol group did not appear at 640 cm^{-1}. [4] The data can be found in Figure B1 (Appendix B) and is similar to previous studies [5,6,7]

The thermal degradation of Poly(p-phenylene vinylene) PPV is shown in Figure 6.1.

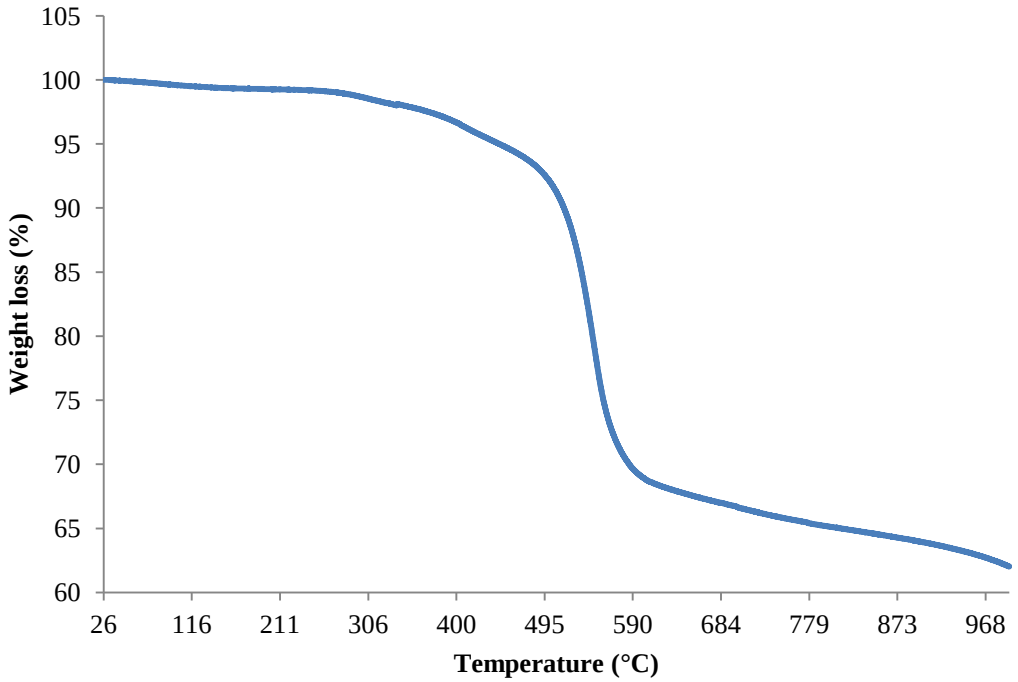

Figure 6.1: TGA data showing the thermal degradation of Poly(p-phenylene vinylene)

The TGA shows the transition temperature of the polymer occurring at around 491-570 °C which is attributed to the decomposition of the polymer which was similar to the results obtained from previous studies. [6, 7]

6.2 Casting of Polydimethylsiloxane films

Table 3.2 shows the effect of dibutyltin dilaurate and TEOS on the viscosity of the PDMS film. PDMS films were cured inside vials with various concentrations of TEOS and dibutyltin dilaurate. After synthesis, the vials were turned upside down and the time for the PDMS to flow down the vial was recorded.. Figure 6.2 shows the vials after being left upside down. The time it took for each sample to drop down the vial was recorded and is shown in Table 6.2. Sample 1 and 2 took 25 and 300 seconds respectively. These results showed that the presence of a catalyst is required to make the mixture more viscous. It can be observed that sample 3 did not flow down to the bottom of the vial but rather halfway and as a result was less viscous than sample 4, 5 and 6. While sample 4, 5 and 6 showed a cured PDMS polymer, the results suggest that the conditions required to synthesize sample 4, 10% TEOS cross linking agent with 1% Dibutyltin Dilaurate were sufficient to synthesize a PDMS elastomer.

Table 6.2: Effect of TEOS cross linker and dibutyltin dilaurate catalyst on polydimethylsiloxane

Sample	PDMS (g)	TEOS (Weight %)	Dibutyltin Dilaurate (Weight %)	Time to drop (seconds)
1	1	1	0	25
2	1	1	1	300
3	1	5	1	N/A
4	1	10	1	N/A
5	1	50	1	N/A
6	1	5	5	N/A

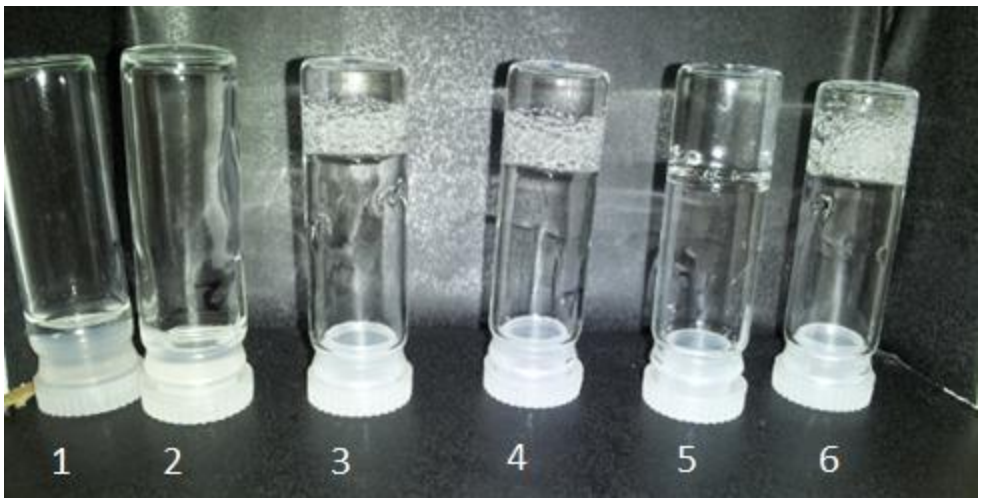

Figure 6.2: Varying concentrations of TEOS and dibutylin dilaurate on PDMS films.

PDMS composite films were synthesized based on the results from Table 6.2. Figure 6.3 shows four different PDMS films and the concentrations of their fillers: PPV/PDMS-10 wt. %, MWNT/PDMS-5 wt. %, MWNT/PDMS-15 wt. %, MWNT/PDMS-25 wt %.

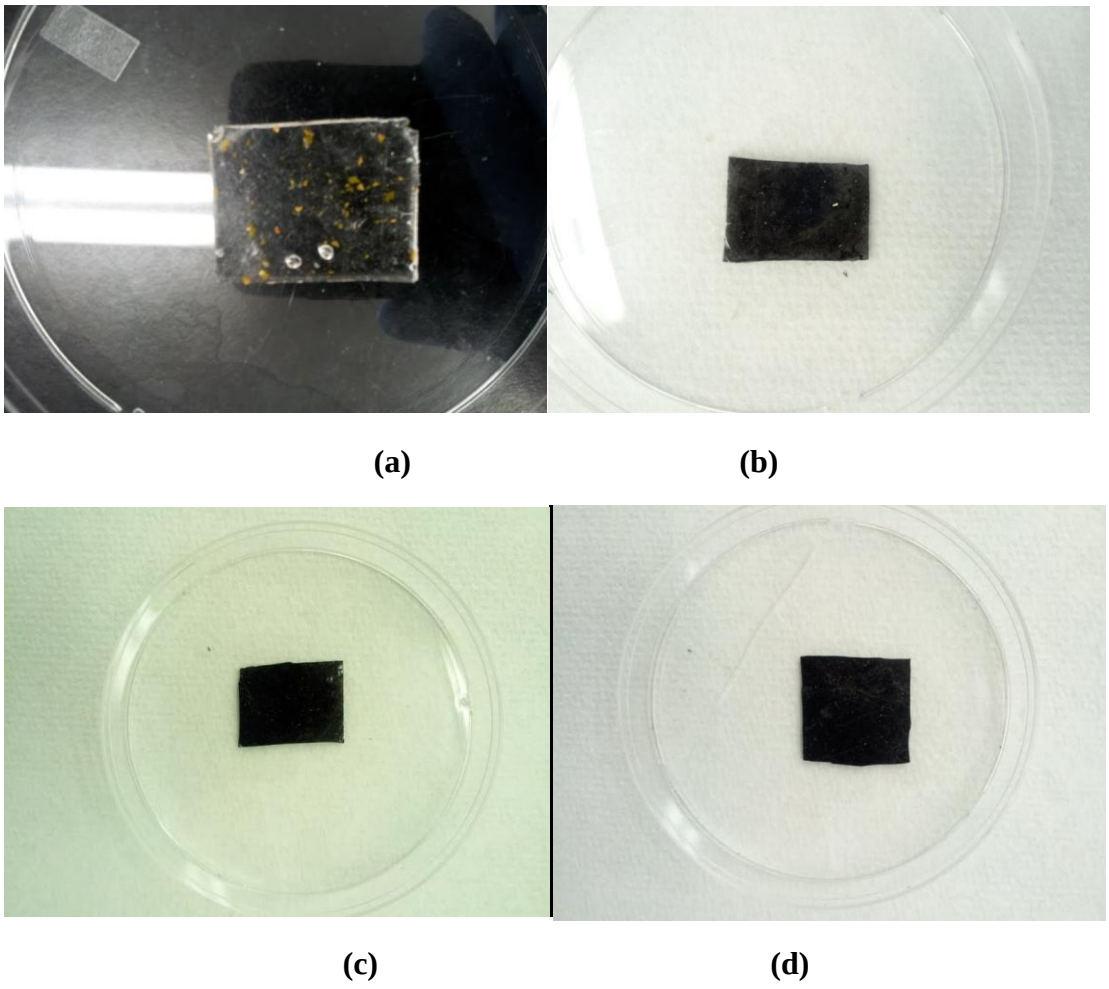

Figure 6.3: PDMS composite films with different filler compositions: (a) PPV/PDMS-10 wt. %, (b) MWNT/PDMS-5 wt. %, (c) MWNT/PDMS- 15 wt. % and (d) MWNT/PDMS-25 wt.%

References

[1] Briquet, F., Colas, A., & Thomas, X. (1996). Silicones for medical use. *12th Technical Conference Polymers for Biomedical Use* (pp. 1-11). Le Mans, France.

[2] Dow Corning Corporation (1997). An Overview of Polydimethylsiloxane (PDMS) Fluids in the Environment. *Science*, 1-2

[3] Uc, Z. K., & East, M. (2003). Synthesis, Characterization and Electrical Conductivity of Poly (p-phenylene vinylene). *Turkish Journal of Chemistry*, *27(2)*, 135 - 143.

[4] Fernandes, M.R.; Garcia, J.R.; Schultz, M.S.; Nart, F.C. (2005). Polaron and bipolaron transitions in doped poly(p-phenylene vinylene) films. *Thin. Solid. Films*, 474(1-2), 279–284

[5] Gagnon, D.R.; Capistran, J.D.; Karasz, F.E.; Lenz, R.W. (1984). Molecular orientation and conductivity in highly drawn poly(p-phenylene vinylene). *Synthetic Materials*., 20(1), 85-95.

[6] Thongchai, N., Kunanuruksapong, R., Niamlang, S., Wannatong, L., Sirivat, A., & Wongkasemjit, S. (2009). Interactions between CO and Poly(p-phenylene vinylene) as Induced by Ion-Exchanged Zeolites. *Materials*, *2*(4), 2259-2275.

[7] Niamlang, S., & Sirivat, A. (2008). Dielectrophoresis force and deflection of electroactive poly(p -phenylene vinylene)/polydimethylsiloxane blends. *Smart Materials and Structures*, *17*(3), 1-9

Conclusion and Future Work

In the second part of this thesis a biocompatible PPV/PDMS and MWNT/PDMS elastomer that has the potential to be used in a cardiovascular application was synthesized. Several conductive polymers and nanotube composites have been synthesized with the following compositions of MWNTs: PPV/PDMS-10 wt. %, MWNT/PDMS-5 wt. %, MWNT/PDMS-15 wt. % and MWNT/PDMS-25 wt %.

Future studies will include coupling a dynamic mechanical analyzer with a current source to understand the effect on the force required to stretch the film a particular length in the presence of an electric current.

General Conclusion

In the first part of this thesis, the synthesis of a cationic hyperbranched phosphorylcholine polymer via RAFT polymerization was described. Different cross-linkers were studied and it was found that with the incorporation of *N*,*N*'-Methylene-bis-acrylamide, copolymers with broad molecular weight distributions greater than 1.5. The hyperbranched cationic phosphorylcholine copolymer was able to condense DNA at varying polymer/DNA mass ratios and as a result had the potential to be used a non-viral gene delivery vector. The transfection efficiency of the copolymers was evaluated by their gene expression in Hep G2 cells. By dissolving the polymers in a $CaCl_2$ solution, the gene expression was significantly improved but was still not comparable to the standard polyethyleneimine. Future work will look into understanding the barriers which prevent the hyperbranched phosphorylcholine polymer from showing high gene expression.

In the second part of this thesis PPV was synthesized and characterized. Subsequently, the PPV together with MWNTs at different compositions were embedded into the elastomer Polydimethylsiloxane. The resulting composite films will be tested for an electro-stiffening effect through the coupling of a dynamic mechanical analyzer and a power source.

Appendix A

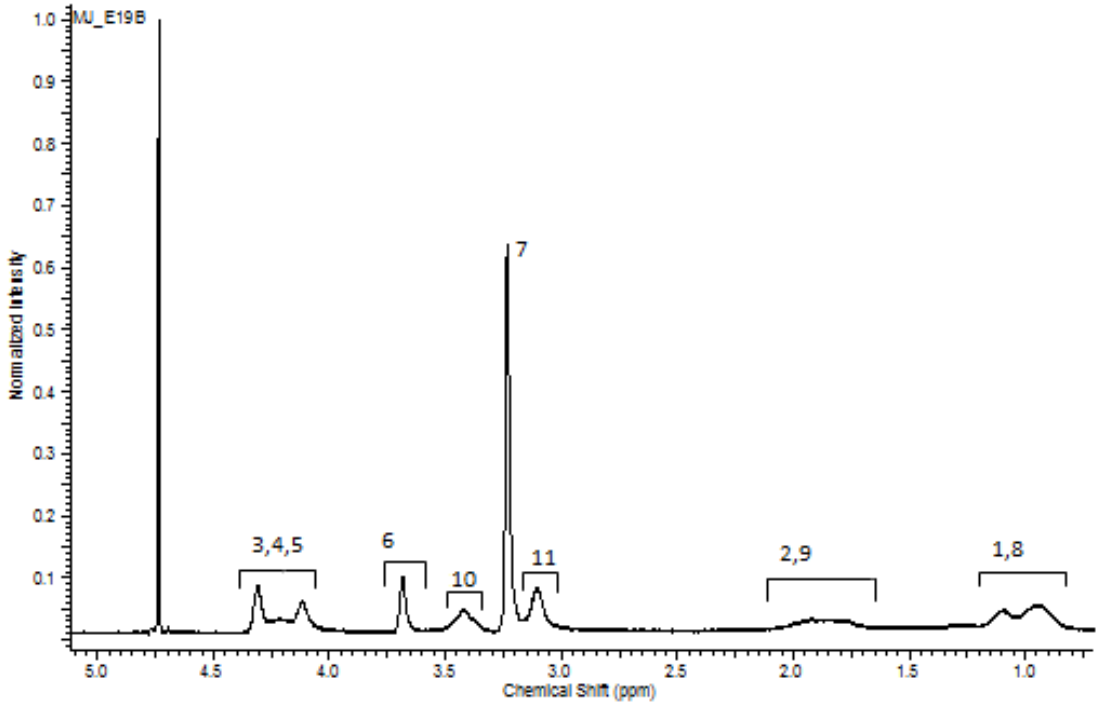

Figure A1: Assigned ^{1}H-NMR spectra for poly(MPC-*stat*-AEMA)

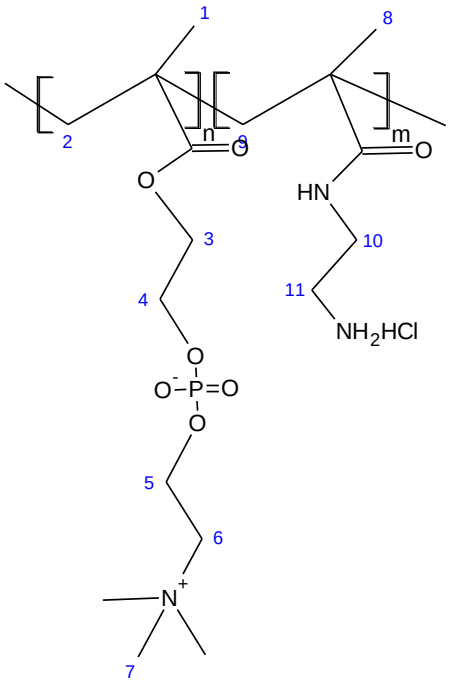

Figure A2: Structure of poly(MPC-*stat*-AEMA)

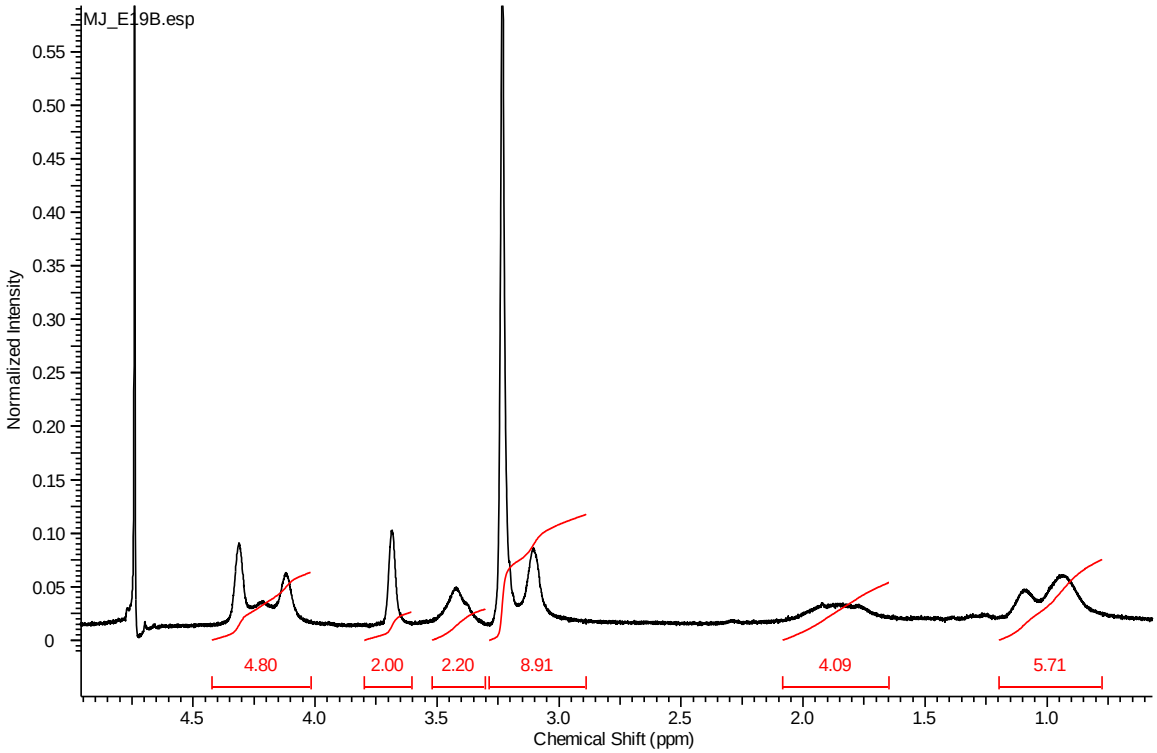

Figure A3: ^{1}H-NMR molar spectra for poly(MPC$_{0.77}$-*stat*-AEMA$_{1.22}$)

Appendix B

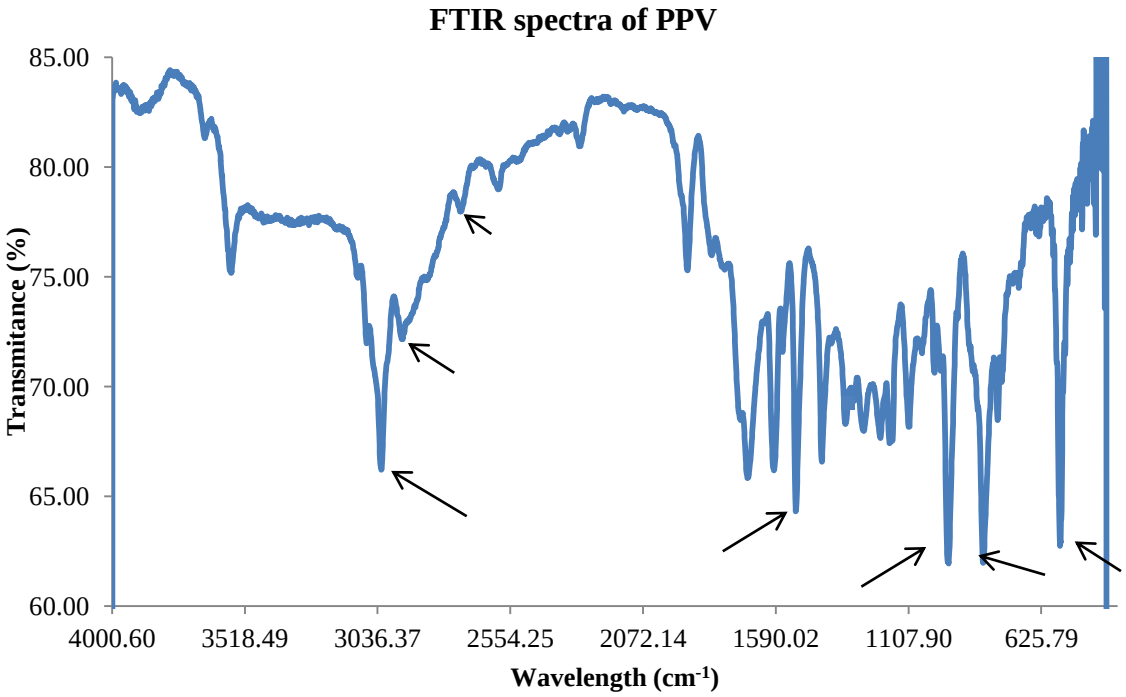

Figure B1: FTIR spectra of PPV